

NASA/TM—2018-219749



BLAYER User Guide

*David A. Saunders and Dinesh K. Prabhu
Analytical Mechanics Associates, Inc.
Aerothermodynamics Branch*

National Aeronautics and
Space Administration

*Ames Research Center
Moffett Field, CA*

January 2018

Since its founding, NASA has been dedicated to the advancement of aeronautics and space science. The NASA scientific and technical information (STI) program plays a key part in helping NASA maintain this important role.

The NASA STI program operates under the auspices of the Agency Chief Information Officer. It collects, organizes, provides for archiving, and disseminates NASA's STI. The NASA STI program provides access to the NTRS Registered and its public interface, the NASA Technical Reports Server, thus providing one of the largest collections of aeronautical and space science STI in the world. Results are published in both non-NASA channels and by NASA in the NASA STI Report Series, which includes the following report types:

- **TECHNICAL PUBLICATION.** Reports of completed research or a major significant phase of research that present the results of NASA Programs and include extensive data or theoretical analysis. Includes compilations of significant scientific and technical data and information deemed to be of continuing reference value. NASA counterpart of peer-reviewed formal professional papers but has less stringent limitations on manuscript length and extent of graphic presentations.
- **TECHNICAL MEMORANDUM.** Scientific and technical findings that are preliminary or of specialized interest, e.g., quick release reports, working papers, and bibliographies that contain minimal annotation. Does not contain extensive analysis.
- **CONTRACTOR REPORT.** Scientific and technical findings by NASA-sponsored contractors and grantees.

- **CONFERENCE PUBLICATION.** Collected papers from scientific and technical conferences, symposia, seminars, or other meetings sponsored or co-sponsored by NASA.
- **SPECIAL PUBLICATION.** Scientific, technical, or historical information from NASA programs, projects, and missions, often concerned with subjects having substantial public interest.
- **TECHNICAL TRANSLATION.** English-language translations of foreign scientific and technical material pertinent to NASA's mission.

Specialized services also include organizing and publishing research results, distributing specialized research announcements and feeds, providing information desk and personal search support, and enabling data exchange services.

For more information about the NASA STI program, see the following:

- Access the NASA STI program home page at <http://www.sti.nasa.gov>
- E-mail your question to help@sti.nasa.gov
- Phone the NASA STI Information Desk at 757-864-9658
- Write to:
NASA STI Information Desk
Mail Stop 148
NASA Langley Research Center
Hampton, VA 23681-2199

Table of Contents

	Page
Abstract	4
Nomenclature	4
I. Introduction	5
II. Inputs and Outputs	5
III. Background	9
IV. Methodology	10
V. Validation	17
VI. Anomalous Behaviors	23
VII. Acknowledgments	28
VIII. References	28

BLAYER User Guide

David Saunders* and Dinesh Prabhu*

A software utility employed for post-processing computational fluid dynamics solutions about atmospheric entry vehicles is described as a supplement to the documentation within the source code. This BLAYER application and its ancillary utilities are in the public domain at <https://sourceforge.net/projects/cfdutilities/>. BLAYER was developed at NASA Ames Research Center in support of the DPLR (Data Parallel Line Relaxation) flow solver. Its underlying algorithm has since been incorporated by others into the LAURA and Us3D flow solvers at NASA Langley Research Center and the University of Minnesota respectively. The essence of the algorithm is to locate the boundary layer edge by seeking the *peak curvature* in a total enthalpy profile. Turning that insight into a practical tool suited to a wide range of possible profiles has led to a *hybrid two-stage method*. The traditional method—location of (say) 99.5% of free-stream total enthalpy—remains an option, though it may be less robust.

Nomenclature

C_H	= film coefficient or heat transfer coefficient, $W m^{-2} K^{-1}$
$f(t)$	= normalized total enthalpy ratio, nondimensional
H	= total enthalpy, $J kg^{-1}$
i,j,k	= grid point index
k	= average surface roughness height, m
K	= degrees Kelvin
m	= meters
M	= Mach number
Pa	= Pascals
q_w	= heat flux at the wall, $W m^{-2}$
q_{vw}	= catalytic heat flux at the wall, $W m^{-2}$, for 2-temperature flow solutions
Re_θ	= Reynolds number based on momentum thickness θ
Re_{kk}	= Reynolds number based on roughness height k (but viscosity at the wall)
Re_{ue}	= unit Reynolds number based on edge conditions
t	= arc length from the wall along a (possibly normalized) flow profile, m or nondimensional
T	= translational temperature, K
T_v	= vibrational temperature, K
v	= velocity, $m s^{-1}$
x,y,z	= Cartesian coordinates, m
γ	= ratio of specific heats, C_p/C_v (heat capacities at constant pressure and constant volume)
δ	= boundary layer thickness, m
δ^*	= displacement thickness, m
δ_u	= velocity thickness, m
ε	= emissivity, nondimensional
θ	= momentum thickness, m
ρ	= density, $kg m^{-3}$
σ	= Stefan-Boltzmann constant, $W m^{-2} K^{-4}$
τ	= shear stress, Pa or force/unit area
κ	= curvature of a (normalized) profile, t^{-1} , or total thermal conductivity, $W m^{-1} K^{-1}$
μ	= viscosity, $Pa s$

* Senior Research Scientist, AMA, Inc. at NASA Ames Research Center, Moffett Field, CA 94035

Subscripts

c	= compressible
$e, edge$	= boundary layer edge value
inc	= incompressible
mod	= moderated
tan	= tangential component (parallel to the wall)
$w, wall$	= wall surface value
∞	= free-stream value

I. Introduction

BLAYER is one of many software utilities developed by the Aerothermodynamics Branch at NASA Ames Research Center in support of flow calculations performed on multiblock structured computational grids. It reads a volume dataset extracted from a flow solution, in either TECPLOT^[1] or PLOT3D^[2] format, and writes a surface dataset in TECPLOT format containing either two or three sets of values: (1) wall data, (2) boundary layer edge-related data, and (optionally) a third set of values either at a specified surface roughness height k or at the estimated momentum thickness height, θ . Post-processing of 2-D and 3-D laminar solutions is commonly performed with BLAYER to predict likely transition to turbulent flow via correlations involving Re_θ or Re_{kk} .

Section II reproduces control input descriptions from the BLAYER source code, and documents the various outputs likewise. The initial implementation dates from 2004, and Section III provides some of the history and other background information. Details of the edge detection procedure (with a choice between a two-stage hybrid method and the traditional 99.5% method plus two choices of boundary layer profile) are provided in the Methodology Section IV. Computed results are compared with those from flat plate theory in Validation Section V along with a study of axisymmetric results for a hemisphere in air and illustrations of 3-D results in air and in the Martian atmosphere. A final Section VI presents examples of behavior on less-than-ideal boundary layer profiles observed by the authors. The utility is robust enough that plottable results can be expected from any likely flow solution, even in separated flow regions, with the proviso that meaningful results will be confined to steady, attached flow.

II. Inputs and Outputs

The main assumptions made in BLAYER are appropriate for hypersonic flow solutions on structured multiblock grids, as follows:

- The grid consists of a single layer of structured blocks in PLOT3D or TECPLOT format.
- The radial grid lines are sufficiently normal to the surface (at least in the boundary layer region) for the 1-D edge detection method to treat grid arc lengths as wall distances.
- The flow quantities are given in SI units at the grid points, not at cell centers.
- The flow may be 2-D or 3-D. This is determined automatically. Internally, 2-D arrays are treated as if they are dimensioned (1:ni,1,1:nk).
- The flow solution BC at the wall is expected to be radiative equilibrium. If not, the output surface heat flux will be invalid. For example, cold wall cases (constant T_w) will produce constant q_w .
- The flow is not adiabatic at the wall, because enthalpy profiles should have zero gradient there.

Note that the wall surface is expected to be at $k = 1$, or $j = 1$ for the 2-D case. By default, the utility finds the face or edge of each grid block with the smallest average initial increment off it, and if necessary permutes the block to put the wall at the $k = 1$ position. Overriding this wall detection is possible and may be necessary—see the optional control file **blayer.inp.2** below. This file can also be used to suppress

processing of certain blocks. For blanked blocks, the surface coordinates are output and all function values are set to 1. Such blocks are retained in the output zones so as not to alter their numbering.

BLAYER processes one grid block at a time, and each radial line is processed independently. The input volume dataset may be TECPLOT ASCII with variable names as shown in two forms below, or PLOT3D formatted or unformatted (for which a means of entering variable names is an option—see control file **blayer.inp.3** below). For large meshes, the PLOT3D/unformatted option is highly recommended. Such files are recognized by requiring use of grid file names ending in .g or .gu. Then the same names are expected for the corresponding *.f or *.fu files.

The output results are in TECPLOT ASCII or binary format, one surface zone per grid block in two or three groups: wall values, boundary layer edge values, and (if $k > 0$ is specified) roughness height k values. An optional additional output, **blayer_edge_surface.dat**, containing boundary layer edge coordinates and thicknesses may occasionally be requested to visualize the computed edge surface. See Fig. 1.

Integral quantities **displacement thickness** (δ^*), **momentum thickness** (θ), and **velocity thickness** are computed via quadrature of nonmonotonic (plain Hermite) local splines vs. radial grid line arc length, using tangential components of velocity (parallel to the wall) at the boundary layer edge δ . The formulations appear on page 14.

BLAYER Control File (Standard Input):

```
TITLE
INPUT VOLUME DATASET
volume.gu          ! Tecplot ASCII or ***.g|***.gu PLOT3D ASCII|binary
OUTPUT TECPLOT FILE
blayer.dat         ! Wall and boundary layer edge results
2                 ! 1 = DATAPACKING=POINT; 2 = DATAPACKING=BLOCK
MISCELLANEOUS CONTROLS
0                 ! Edge method: three choices are explained below
0.85              ! Emissivity (0.89 = RCG everywhere)
0.001524         ! Roughness ht. k, m (=0.060" for Orion) |0|-1|-2
0 1 1           ! Block #, i, j for sample H/Hinf & Re-kk profiles
5               ! # species      [5 if omitted]
1              ! # temperatures [1 if these numbers are omitted]
0             ! # extra items  [0 " " " " " " ]
0.           ! Optional input for Hinf > 0. | blk. 1 1,1,nk value
98.          ! Optional %H/Hinf > 0. value for Hignore | 95%
0.           ! Optional Hshift if > 0. (e.g., Hform(OK) for CO2)
```

See below for the extended use of the **datapacking** control to invoke an optional second output file.

Edge method (EM) Extended Usage:

```
EM  >= 0.  means use the enthalpy ratio (H + Hshift) / (Hinf + Hshift)
EM  < 0.   means use the enthalpy ratio (H - Hwall) / (Hinf - Hwall)
|EM| < 90. means use the hybrid curvature-based method
|EM| = 99.5 means use the traditional 99.5% method (or 99. or whatever)
Thus EM = 99.5 means hybrid with Hshift profile (H/Hinf for air/Hshift=0.)
EM = -1.  means hybrid with Hwall profile
EM = -99. means traditional 99% method with Hwall profile
```

Roughness height control k has multiple uses as follows:

```
k = 0.  means suppress the third set of results
k > 0.  means normal usage for a height in meters
k + 20. means replace  $\delta^*$  (displacement thickness) with velocity thickness
        while also outputting results for roughness height k
k = -1. means output results at height  $\theta$  (momentum thickness) and  $Re_\theta$  instead
        of  $Re_{kk}$ 
k = -2. means the same as -1. but output  $Re_\theta M_{edge}$  instead (use if  $M_{edge} > 1?$ )
k = -21. means the same as -1. but replaces  $\theta$  with velocity thickness
k = -22. means the same as -2. but replaces  $\theta$  with velocity thickness
```

Note that Re_θ can also be obtained within TECPLOT by multiplying unit Reynolds number Re_{ue} with θ . Re_{ue} is the unit Reynolds number based on edge conditions. Re_{kk} is Reynolds number based on roughness height k and conditions at that height but using viscosity at the wall rather than at k .

Hinf controls how the total enthalpy ratio in each profile is normalized as follows:

Hinf > 0. \Rightarrow use that value to normalize all profiles
 Hinf = 0. \Rightarrow use the value from block 1, point (1,1,nk) [default]
 Hinf = -1. \Rightarrow use the (i,j,nk) value for profile (i,j) of each block
 Hinf = -2. \Rightarrow use the peak value along each profile (for arc-jet solutions?)

Hignore is the enthalpy ratio value below which profile data are ignored—i.e., the point at which to start the search for the boundary layer edge. The default is 95%, but for Orion this has been found to encounter another heuristic affecting the upper end of the search region. Therefore, 98% is now the recommended choice. (For the Shuttle OMS pod, even 95% misses the much more likely edge estimate that 50% will find.) Note that this control may affect another heuristic that determines where to stop short of possible shock-related anomalies in the far end of a profile.

Hshift is discussed on p. 11. It should be zero for solutions in air, but was prompted by calculations for Mars. It is ignored if the edge method is negative, meaning use the profile $(H - H_{wall}) / (H_\infty - H_{wall})$.

Option Ancillary Control File, **blayer.inp.2**

Line 1 may be used to suppress processing of some blocks; a blank line means process all blocks.

Lines 2+ may be used to override the automated wall detection scheme, one block per line.

For example:

```
10 12 14:18      means blank blocks 10, 12, 14, 15, 16, 17, 18      (any intelligible integer list works)
2 5              guarantees that for blocks 2, 3, 4, face 5 (k = 1) is the wall
3 5
4 5
```

Option Ancillary Control File, **blayer.inp.3**

This option was prompted by the need for handling input volume datasets in PLOT3D form. Line 1 should contain all species names. If extra flow variables are present, their names should appear on line 2. For example:

```
n2 o2 no no+ n2+ o2+ n o n+ o+ e
Cp N_tot
```

If either line is empty (or this control file is missing), the variable names are defaulted as follows:

```
sp_1 sp_2 sp_3 ... sp_11
xtra_1 xtra_2
```

Input Volume File Format (1): TECPLOT ASCII

```
TITLE      = ""
VARIABLES = "x, m"
"y, m"
["z, m"      for the 3-D case]
"rho, kg/m^3" density
"p, Pa"     pressure
"T, K"      translational temperature
["Tv, K"    vibrational temperature; the default is 1 temp.]
"c_N_2"     1 or more species densities
"c_O_2"
```



```

"c_N_O"
"c_N"
"c_O"
["::: more species if specified; the default is 5 species]
"u, m/s" velocity components
"v, m/s"
["w, m/s"] for the 3-D case
"H0, J/kg" total enthalpy
"M" Mach number
"mu, Pa.s" viscosity
["kappa, W/m.K" total thermal conductivity if # temperatures > 1]
["::: miscellaneous extras; the default is 0 extras]
ZONE T="Zone 1"
I=17, J=25, [K=81, ]ZONETYPE=Ordered
DATA PACKING=BLOCK
DT=(DOUBLE DOUBLE ..... DOUBLE DOUBLE )
6.64733315E+00 6.57563824E+00 6.48970469E+00 6.39077472E+00 6. ...
: : : : :

```

Also, the format written by the DPLR^[3] postprocessor is handled as in the following example:

```

[Optional title]
variables=x,y,[z,]rho,p,T,C_n2,C_o2,C_no,C_n,C_o,u,v,[w,]h,M,mu
zone t="flow2|3d" F=point, i= 161 j= 157 k= 1|81
6.64733315E+00 6.57563824E+00 6.48970469E+00 6.39077472E+00 6. ...
: : : : :

```

Input Volume File Format (2): PLOT3D Formatted or Unformatted

As mentioned above, the unformatted option here produces significantly better I/O performance for large grids. The input volume grid file name should end in .gu. For DPLR users, the POSTFLOW control file should use output format 3, and the following flow variable codes

```

ivarp = 0 100 110 120 1000 10 151 [152] 132 154 50 [extras] or
ivarp = 0 100 110 120 125 1000 150 151 [152] 132 154 50 52 [extras]

```

for single-temperature and two-temperature solutions, respectively, analogous to the above TECPLOT format.

Output Results (TECPLOT ASCII or Binary): One Zone Per Grid Block

The columns below represent surface datasets of results at the wall, results at the boundary layer edge, and (unless $k = 0$ is specified) results at roughness height k or (if $k < 0$ is specified) at height θ (momentum thickness).

Wall	Boundary layer edge	Roughness height ($k \neq 0$)
x	density	height k
y	pressure	density
s z	temperature	velocity
density	total enthalpy	viscosity
pressure	u	Re-kk
temperature	v	
[Tw]	[w]	or (if $k = -1.$ or $-2.$):
total enthalpy	Mach number	
viscosity	viscosity	Theta height values
N2 species density	N2 species density	
O2 " "	O2 " "	k (= theta)
NO " "	NO " "	density at theta
N " "	N " "	velocity at theta
O " "	O " "	viscosity at theta
[?? " "]	[?? " "]	Re-theta (k = -1.)
heat flux	delta	Re-theta/Medge (= -2.)
tau_x	delta* or vel-thickness, depending on input k	
tau_y	theta	(see more on k above)
[tau_z]	Re-ue	
[kappaw]	CH	
[extras]	[kappae]	
	[extras]	

Note that the 2-D case writes running length s (along the wall from the upstream edge of the current block) in place of coordinate z . This starts at zero for each block, though. Also, a SORT_SURFACE_SLICE utility is available from the present author to determine cumulative surface arc lengths across block boundaries from a 3-D solution sliced (within TECPLOT) at (say) $y = 0.001$ m for a symmetry plane cut.

Optional Additional Output File (TECPLOT ASCII): `blayer_edge_surface.dat`

A user request led to retrofitting of optional output of a plottable file containing boundary layer surface coordinates and thicknesses via the output **datapacking** control: 21 or 22 produces structured zones (in point order for this formatted file) while functioning as for 1 or 2 otherwise (point or block order for the main output file). Figure 1 shows an example.

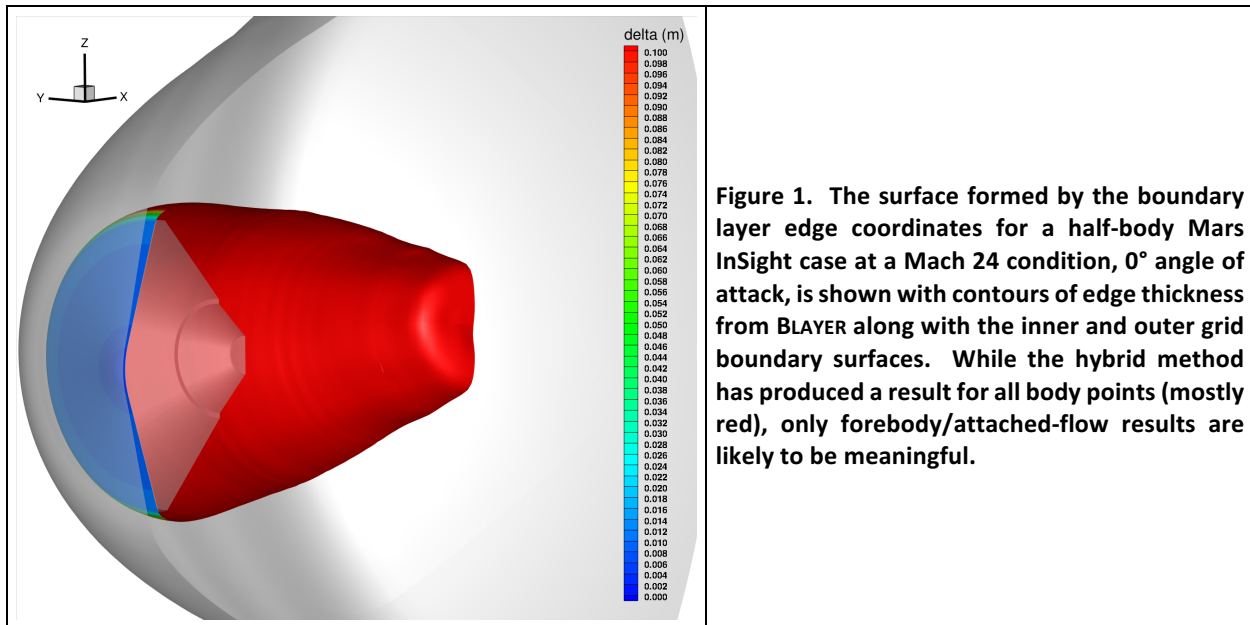


Figure 1. The surface formed by the boundary layer edge coordinates for a half-body Mars InSight case at a Mach 24 condition, 0° angle of attack, is shown with contours of edge thickness from BLAYER along with the inner and outer grid boundary surfaces. While the hybrid method has produced a result for all body points (mostly red), only forebody/attached-flow results are likely to be meaningful.

III. Background

The boundary layer at the surface of an atmospheric entry vehicle is the region where the enthalpy of the free stream flow is being dissipated by viscosity, transferring energy in the form of heat. Real gas Navier-Stokes flow solvers routinely model this phenomenon as part of predicting the aerothermodynamic environments that entry vehicles must be designed to withstand. The importance of knowing boundary layer properties and their relation to possible transition from laminar to turbulent flow is illustrated by Space Shuttle *Discovery* mission STS-114, when the appearance of tile gap filler protrusions on the underside of the nose was deemed serious enough that a crew member was called upon to exit the vehicle and remove the potential threat prior to descent from orbit.^[4]

Hypersonic entry vehicles tend to be fairly simple shapes such as sphere-cones that lend themselves to use of structured computational grids consisting of a single layer of grid blocks. Even the Space Shuttle Orbiter can be gridded this way. Since the grid lines off the body should be perpendicular to the wall, at least in the boundary layer, they in turn lend themselves to direct use for profiles of the appropriate flow solution quantity—total enthalpy (which is conserved across a shock as long as the inviscid part of the shock layer is adiabatic). Thus, entire surface distributions of boundary layer properties can be calculated one surface grid point at a time, either within the flow solver or as a post-processing utility. Such calculations are meaningful for *attached* flow, yet separated flow regions need to be handled gracefully, if only for plotting purposes.

Boundary layer “edge” locations can be affected by the particular choice of boundary layer profile and the associated normalizations. There are at least two choices of total enthalpy profile, and these can produce different calculated edge locations. Derived quantities such as displacement thickness and momentum thickness, on the other hand, should be insensitive to the profile choice, as will be demonstrated in Section IV. This may not be true, though, for profiles with overshoots or undershoots, even on the forebody, as will be illustrated in Section VI.

The BLAYER utility used as part of post-processing flow solutions for Orion/MPCV and other entry vehicles is a generalization of the earlier BLAYER_RESULTS utility developed at NASA Ames Research Center following the STS-107 *Columbia* accident. BLAYER handles 3-D and 2-D/axi-symmetric flows and a variable number of gas species for any atmosphere. It allows for more than one temperature and for optional extra flow quantities, and omits optional handling of Orbiter tile datasets. It produces a surface dataset containing computed values of numerous quantities at the wall and at the boundary layer edge height, and (optionally) certain quantities at a specified surface roughness height k .

IV. Methodology

The traditional approach of defining the boundary layer edge at a given body point as the location nearest to the body of 99% or 99.5% of the free-stream total enthalpy normally suffices for the two-dimensional flows upon which that choice is based. Three-dimensional flow however can, in practice, present boundary layer profiles that may differ significantly from their 2-D counterparts by undershooting or overshooting the free-stream reference value in the region of interest. The total enthalpy ratio H/H_∞ doesn’t necessarily asymptote to 1 near the body. Indeed, enough of an undershoot can mean that the traditional method fails completely. Locating the *peak curvature* along each profile instead as a “knee in the curve” is the approach that has been applied here in pursuit of a more robust edge method. It turns out, though, that curvature can be a vexing quantity to work with, so this idea also presents practical difficulties demanding heuristics that risk being thwarted by odd profiles commonly seen in the wake—not that results from separated flow regions are expected to be meaningful as already indicated.

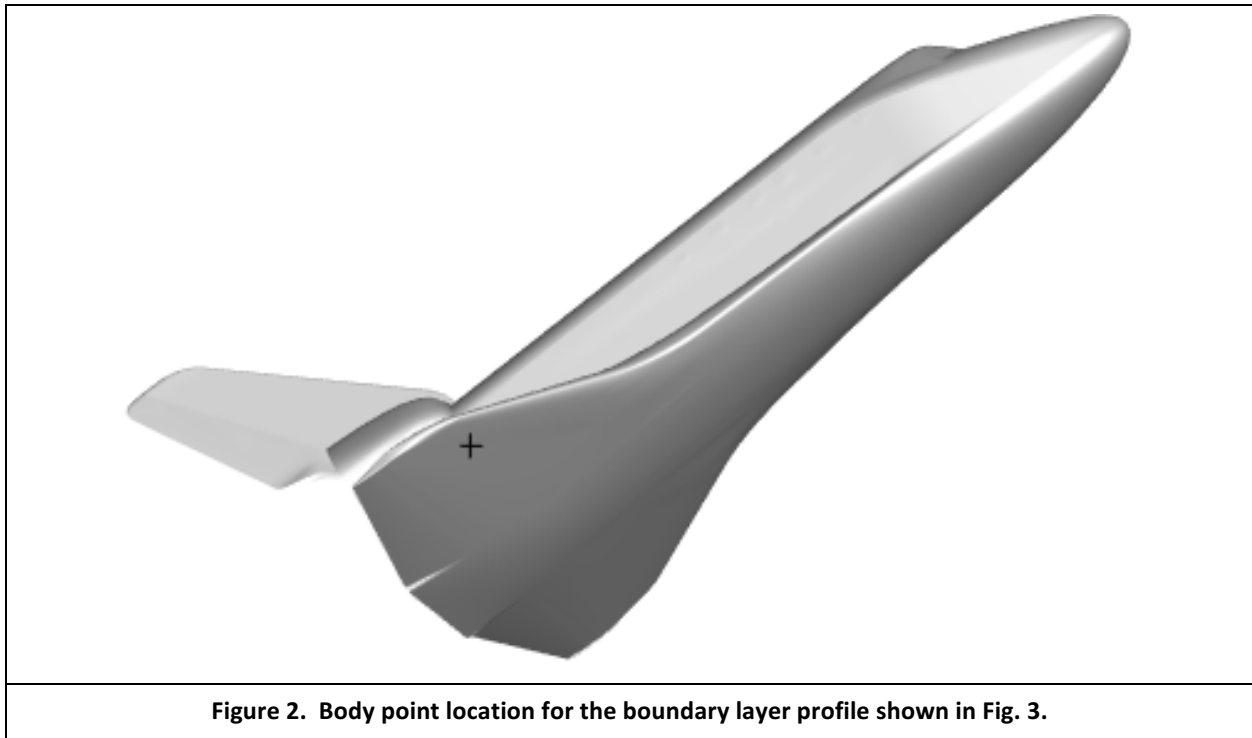
The scheme presently implemented is a *hybrid* method: use a curvature-based scheme to locate the likely neighborhood of the edge in the total enthalpy ratio profile, then apply the 99.5% rule to the *peak ratio in that neighborhood*. For well-behaved profiles, this is consistent with the traditional edge method (which remains a user option). In the presence of overshoots or undershoots, the hybrid method inevitably produces edge thicknesses differing from traditional method results, but plausible results for irregular profiles can be obtained when the traditional method fails.

While total enthalpy is the appropriate profile choice for edge detection in hypersonic flow (and lower speeds), a computed boundary layer edge location is affected by the particular choice of profile. The units need to be nondimensionalized, specially if profile curvatures are being used. The arc length choice in BLAYER is to normalize distances along wall-normal grid lines by the total arc length of the relevant grid line. (Use of a common reference length would have been another reasonable choice.) Initially, total enthalpy was normalized by the free-stream value, as H/H_∞ , which is suitable in air with the DPLR energy reference value choices but not in other atmospheres such as at Mars, where enthalpies can be negative. One choice is to shift all total enthalpies, if necessary, to avoid possible negative values, giving the ratio $(H + H_{shift})/(H_\infty + H_{shift})$. At Mars, the recommended additive shift is 8,932,880.0 J/kg, based on the enthalpy of formation of CO₂ at 0 K. Another (widely preferred) choice is to use the ratio $(H - H_{wall})/(H_\infty - H_{wall})$, and this would affect results even in air. BLAYER supports this option, but it is not in use for Orion/MPCV.

A representative normalized total enthalpy ratio profile from an outer wing grid block on the wind side of a Shuttle Orbiter grid for a Mach 17.88 condition is shown below (Figs. 2 and 3). The hybrid edge method suppresses the outer quarter of points on a wall-normal grid line to avoid shock effects. For the remaining grid points, it first locates the neighborhood of the peak curvature by working with a *smoothed*

and *moderated* form of raw curvature. Raw curvature values are estimated with three-point finite difference first and second derivatives of total enthalpy ratio $f(t)$ vs. normalized distance t as: curvature $\kappa = -f(t)'' (1 + f(t)'^2)^{-1.5}$. The raw curvature distributions tend to be spiky and intractable (Fig. 4, left). They are therefore smoothed with one pass of a local averaging method, then moderated as follows: $\kappa_{mod} = (1 + |\kappa|)^{-0.1}$; if $\kappa < 0$, $\kappa_{mod} \leftarrow 2 - \kappa_{mod}$. A 1-D minimization determines the (preliminary) edge location between data points (Fig. 4, right), but that is now just part of defining a neighborhood for the hybrid scheme as it applies the 99.5% rule to the peak ratio *in that neighborhood*. The peak exceeds 1.0 in the example shown, thus producing an edge height of about 0.04 (normalized units).

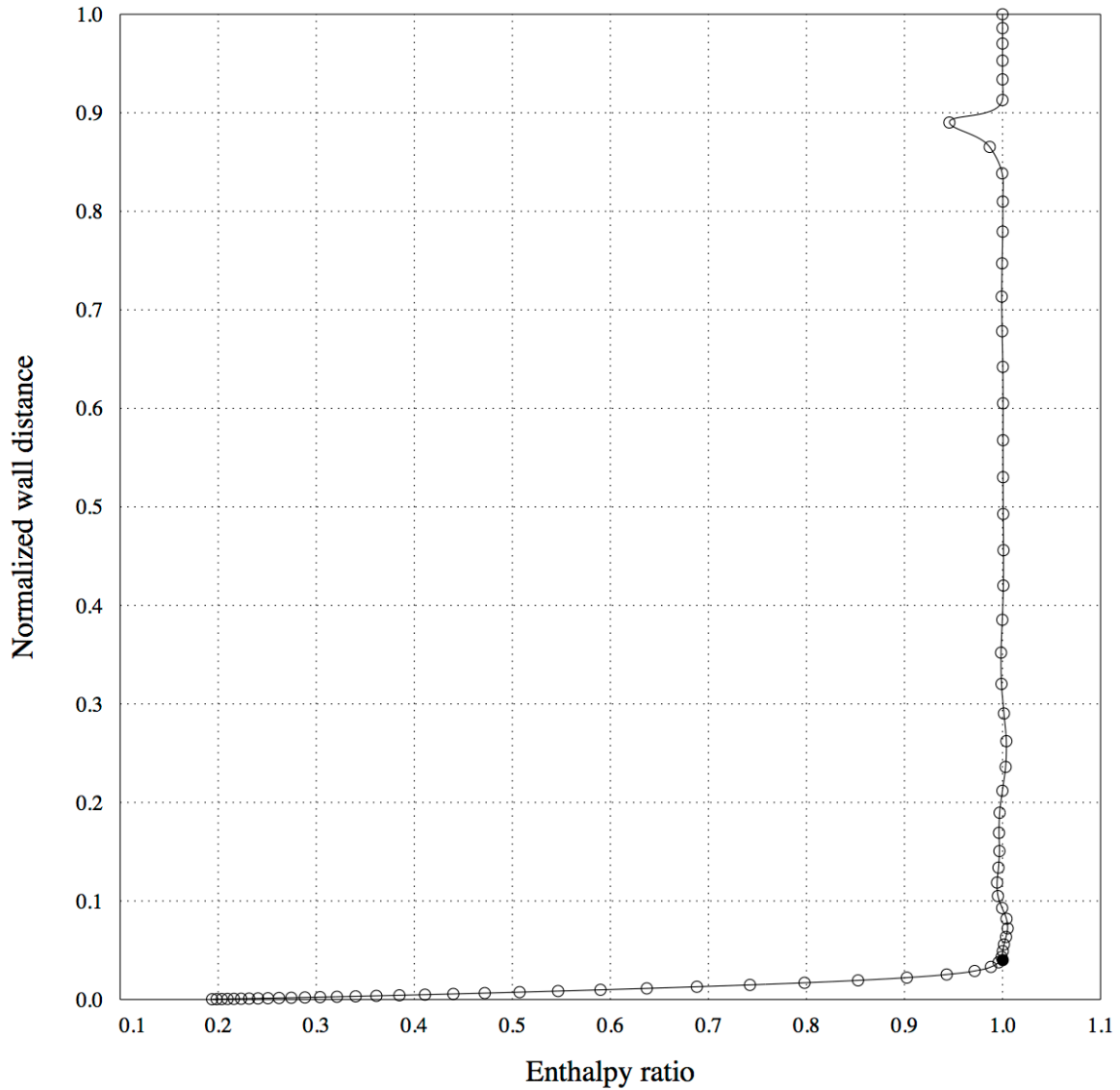
One reason for no longer employing the pure peak-curvature location is that curvature can sometimes be essentially constant or flat in the edge region. The precise peak may lie between indices j and $j+1$ for one profile then between $j+1$ and $j+2$ (say) for a neighboring profile, possibly producing an unlikely jump in the peak-curvature-based edge thickness δ . Even though δ itself is seldom the quantity of interest, its contours should vary more continuously/smoothly than has been observed in the presence of this phenomenon. Thus, the hybrid method derives a larger index range from the carefully computed peak curvature location, then locates where 99.5% of the peak ratio *in that index range* lies via inverse local spline interpolation as a second step.



Shuttle Boundary Layer Profile, Mach 17.88

Block: 38 i: 18 j: 72

● Boundary layer edge is at (1.00024, 0.04005)



File name: log.b38_i18_j72 Plot date: 2006-04-10 @ 14:07

Figure 3. Representative Shuttle normalized boundary layer profile and edge location computed by BLAYER's hybrid method as the point where the total enthalpy ratio is at 99.5% of the *peak ratio in the region of interest*. This neighborhood is initially located via a curvature-based scheme (see Fig. 4).

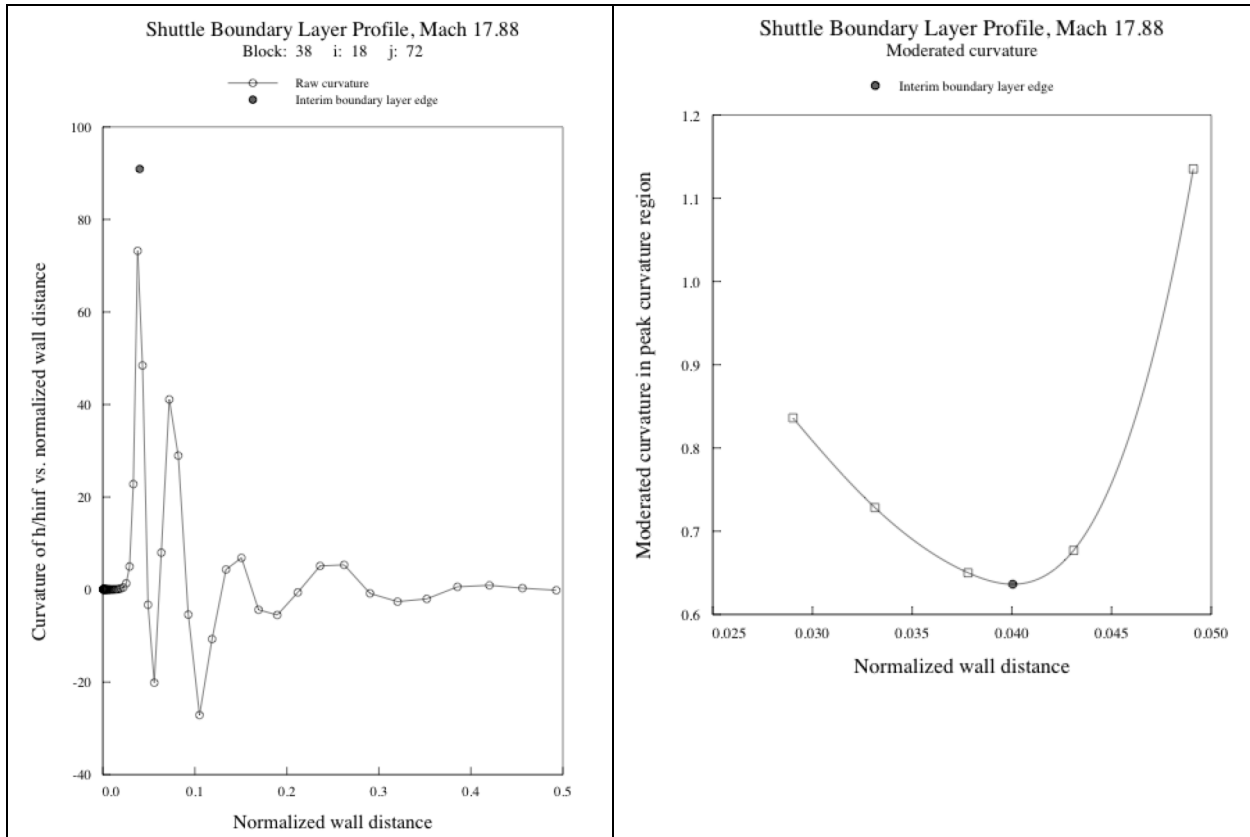


Figure 4. Part of the raw curvature distribution for the profile of Fig. 3 is shown on the left, with a spiky peak that has been moderated as a related function on the right, where an extremum has been estimated precisely between grid points. Originally, the denormalized form of this location was taken to be the boundary layer edge. However, this location is not independent of the choice of profile or its normalizations, so the hybrid method employs only the grid point index nearest to the curvature peak to define an edge neighborhood.

Derived Quantity Formulations: Various wall and edge-related quantities are derived from the underlying flow solution as follows.^[5] Partial derivatives with respect to wall-normal distance are approximated by 2-point finite differencing of profile data points $k = 1$ (wall) and $k = 2$. For example, the unit wall normal vector components are approximated as $(x_2 - x_1)/(t_2 - 0)$, $(y_2 - y_1)/t_2$, and $(z_2 - z_1)/t_2$ where t_2 is the wall-normal grid point 2 distance from the wall. Note that to avoid possible difficulties at a stagnation point, velocities are safeguarded by adding 10^{-10} to them before they are used in the following calculations.

Surface convective heat flux, q_w : Including heat flux in the input volume dataset is not an option with DPLR. The choice that allows BLAYER to include surface heat flux in the output dataset is to assume the radiative equilibrium boundary condition $q_w = \varepsilon \sigma T_w^4$, where ε is the emissivity, σ is the Stefan-Boltzmann constant (originally hard-coded as 5.66097×10^{-8} , although the 2014 value^[6] is $5.670367 \times 10^{-8} \text{ W m}^{-2} \text{ K}^{-4}$), and T_w is the wall temperature, K . For typical arc-jet flow solutions, use of different boundary conditions can mean that BLAYER's q_w output is meaningless. Also, Orion standard practice is for a post-processing script to replace this BLAYER output with the surface heat flux from DPLR. In retrospect, two-point finite differencing at the wall would have been a more general way to provide the surface heat flux.

Catalytic heat flux, q_{v_w} : Two-temperature solutions are expected to include vibrational temperature T_v and total thermal conductivity $\kappa \text{ (W m}^{-1} \text{ K}^{-1}\text{)}$ in the input volume dataset. A catalytic surface heat flux is defined as $q_{v_w} = q_w \text{ (total heat flux)} - \kappa_w (\partial T / \partial t)_w$, where t is arc-length along the body-normal grid line.

Surface Shear Stress, τ : The shear stress vector at the wall is defined as the wall viscosity times the wall-normal derivative of the tangential velocity: $\tau_w = \mu_w \partial v_{tan}/\partial t$ where $v_{tan} = v - v \cdot n$ is the tangential component of velocity at grid point 2 off the wall, n is the wall-normal vector to grid point 2, and v is the velocity vector at grid point 2.

Displacement thickness, δ^* : BLAYER computes several integral quantities with local cubic spline quadrature between the wall and the boundary layer edge using profile data from the wall to the grid point beyond and nearest to the edge location. Displacement thickness (“delstar”) is defined from mass flow rate as:

$$\delta^* = \int_0^\delta \left(1 - \frac{\rho(t)|v_{tan}(t)|}{\rho_{edge}|v_{tan}|_{edge}} \right) dt$$

Momentum thickness, θ : This is also based on mass flow rate:

$$\theta = \int_0^\delta \left(\frac{\rho(t)|v_{tan}(t)|}{\rho_{edge}|v_{tan}|_{edge}} \right) \left(1 - \frac{v_{tan}(t)}{|v_{tan}|_{edge}} \right) dt$$

Velocity thickness, δ_u : This quantity may be substituted for displacement thickness via the roughness height control input, q.v.:

$$\delta_u = \int_0^\delta \left(1 - \frac{|v_{tan}(t)|}{|v_{tan}|_{edge}} \right) dt$$

Unit Reynolds Number, Re_{ue} : The unit Reynolds number based on edge conditions is:

$$Re_{ue} = \frac{\rho_{edge}|v|_{edge}}{\mu_{edge}} \quad Re_{kk} = \frac{\rho_k|v|_k}{\mu_{wall}}$$

Note that the commonly required Re_θ could be obtained from multiplying Re_{ue} and θ at each surface point (within TECPLOT), but alternatives are available. If roughness height $k > 0$ is specified, Re_{kk} is computed using conditions at height k , except that viscosity is taken to be the *wall* value.^[7] If k is entered as -1. or -2., Re_{kk} is replaced by Re_θ or Re_θ/M_{edge} respectively. The latter may be appropriate if $M_{edge} > 1$.

Film coefficient: This quantity is typically required by material response solvers:

$$C_H = \frac{q_w}{(H_{edge} - H_{wall})}$$

Representative profiles and their effects on some of these derived quantities are plotted in Figs. 5-8. Figure 5 illustrates the somewhat different edge results produced by different choices of total enthalpy ratio profile with an example from a calculation for IRVE-2 (Inflatable Reentry Vehicle Experiment) at a Mach 2 condition (axisymmetric). Similar differences are unavoidable with different forms of normalizing the wall distances (such as by a constant reference length for all radial grid lines rather than by the radial grid line arc lengths as here). Thus, the computed edge location is not unique, but as the ensuing figures show, this is not necessarily critical to the integrated quantities, which are barely affected by the choice of profile. The profile in Fig. 5 is at $i = 64$, where $x \sim 0.35$ and $r \sim 0.72$, a little less than halfway along the forebody cone.

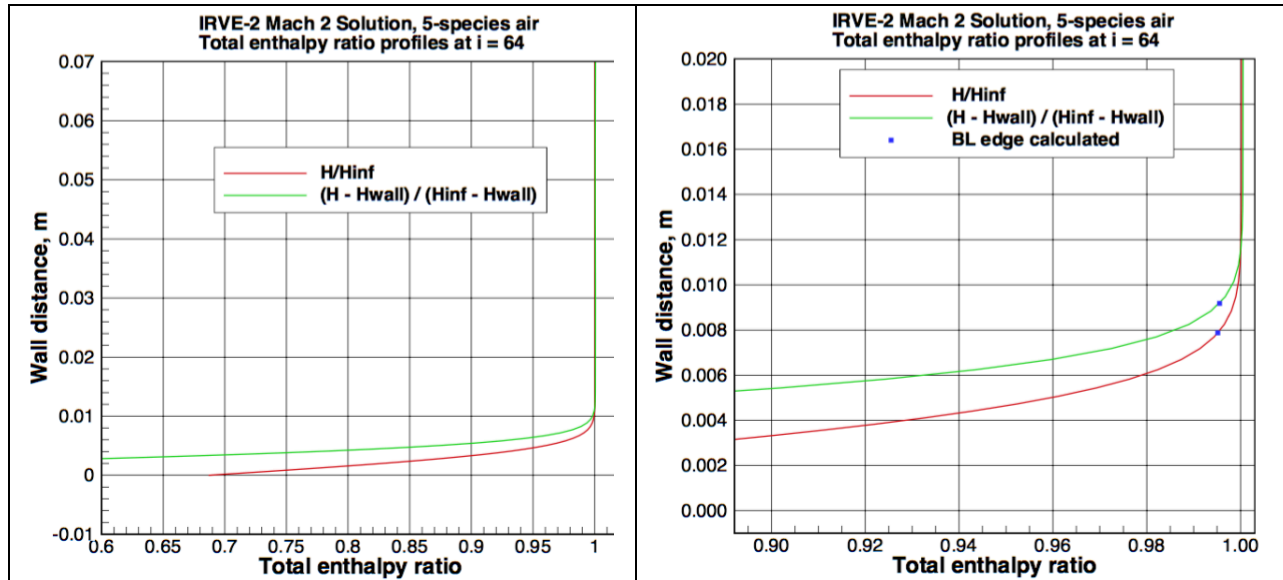


Figure 5. Two forms of the total enthalpy ratio profile are compared for an IRVE-2 body point at Mach 2 in air. The plotted wall distance has been denormalized, and the right-hand plot is a zoom of the left-hand plot. The scales amplify the profile differences. These two forms of the hybrid method produce edge heights that are about 1.3 mm apart on a vehicle that is 3 meters in diameter (0.00784 and 0.00913 m). Database calculations for Orion/MPCV employ the form shown in red.

Figure 6 illustrates the integrands for the profile of Fig. 5 that produce negligibly different values for displacement thickness δ^* and for momentum thickness θ . Note how they asymptote towards zero in the vicinity of the different edge estimates.

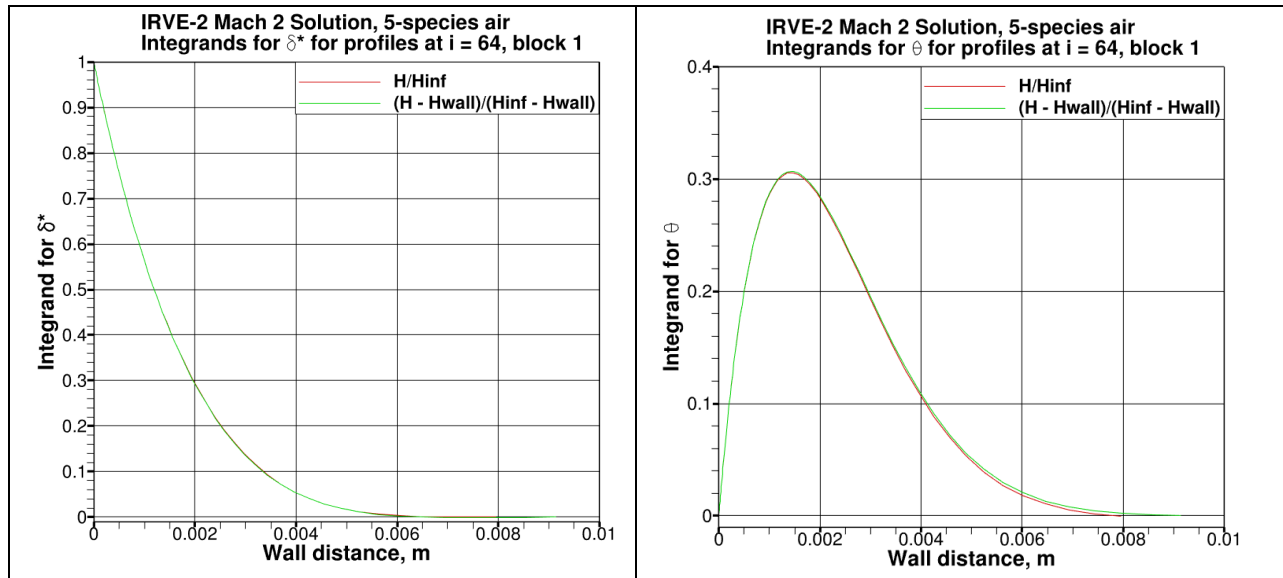


Figure 6. The integrands for displacement thickness δ^* and momentum thickness θ from the two profiles in Fig. 5 are shown to asymptote towards zero and to differ only imperceptibly in spite of the visible difference in computed boundary layer thicknesses at this body point.

The full forebody distributions for edge thickness δ and displacement thickness δ^* are compared in Fig. 7. Note how insensitive the latter is to the choice of total enthalpy ratio.

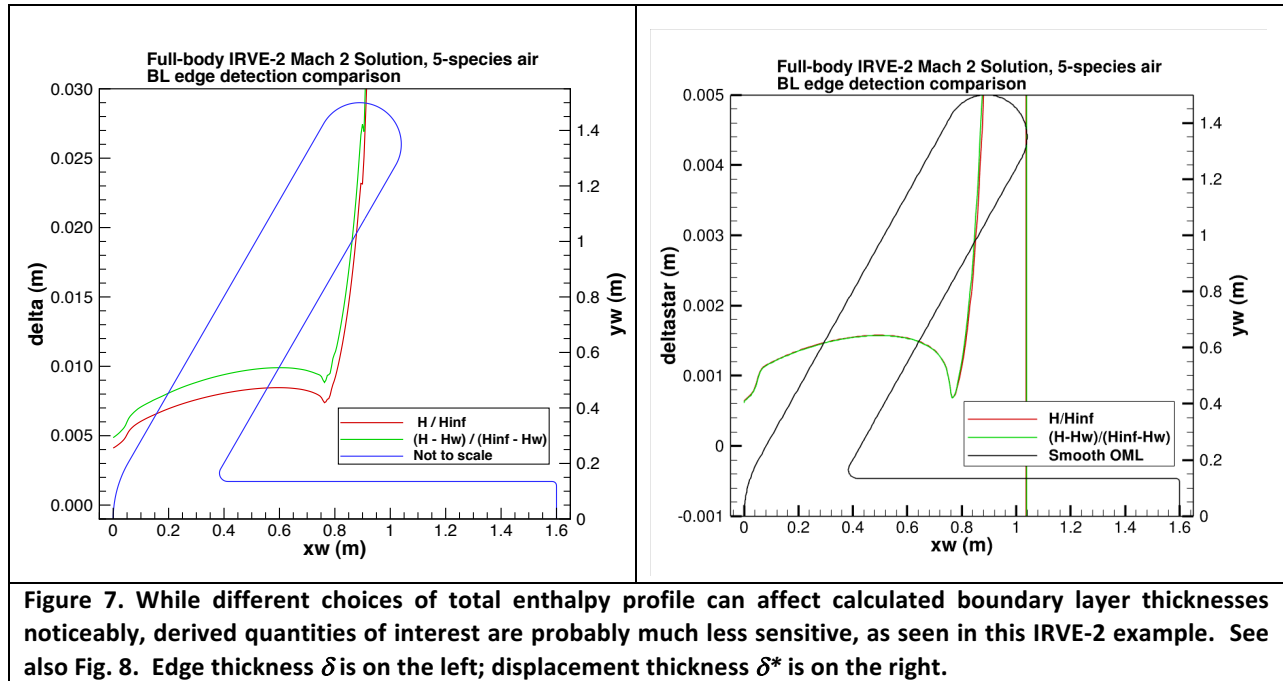


Figure 7. While different choices of total enthalpy profile can affect calculated boundary layer thicknesses noticeably, derived quantities of interest are probably much less sensitive, as seen in this IRVE-2 example. See also Fig. 8. Edge thickness δ is on the left; displacement thickness δ^* is on the right.

Forebody distributions for momentum thickness θ and heat transfer coefficient C_H are compared in Fig. 8. As with δ^* , these are hardly affected by the different choices of total enthalpy ratio. Note that at the stagnation point ($x_w = 0$), the tangential velocity component is zero for the entire profile, producing zeros for δ^* and θ . BLAYER now traps such a finding and replaces the zeros with extrapolations.

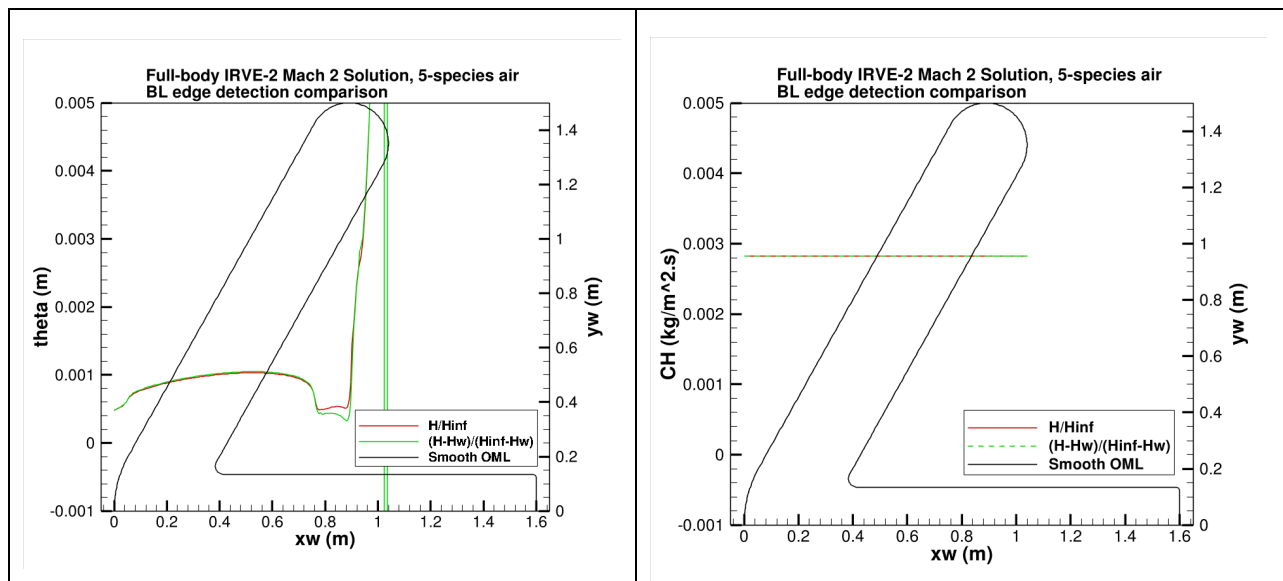


Figure 8. The minimal effect of total enthalpy profile on forebody momentum thickness θ is shown on the left for the forebody of IRVE-2 at the same Mach 2 condition as in Figs. 6-7. Another BLAYER output, heat transfer coefficient C_H , is unaffected by boundary layer edge calculations, and essentially constant on this forebody (right).

V. Validation

Surprisingly, until the present software was initiated following the *Columbia* accident, no similar utility is known to have been in routine use at NASA. This is surely a symptom of writing “research” codes without widespread use in mind and not due to any lack of understanding of boundary layer theory and practice. The original motivation here was to facilitate estimation of Re_θ and Re_{kk} for application to laminar-turbulent transition correlations, and to explore the peak-curvature idea for its potential in improving behavior on 3-D configurations. As indicated above, a computed boundary layer edge is not unique, as it can depend on the choice of profile (the enthalpy-related quantity and the wall distance, both of which are normalized in some way). Initial BLAYER studies simply compared the pure curvature-based edge detection with the traditional 99.5% method, revealing the need for various refinements in order to produce smoothly varying results along the surface, eventually leading to the current hybrid method. A few standard cases are presented here.

Flat Plate Case (2-D planar flow, ideal gas): Steady 2-D incompressible laminar flow with constant viscosity, density and free-stream velocity over a flat plate lends itself to analysis with the Blasius equations, which have been validated against experiment.^[5, 8] Corrections to the equations for compressible flow have also been established.^[9] For a comparison between flat plate theory and computations by DPLR and BLAYER, an example is detailed as follows.

Flat Plate Freestream Conditions & Modeling: $M_\infty = 4$, $T_\infty = 217.8 \text{ K}$, $T_w = 2T_\infty$, $\rho_\infty = 0.029 \frac{\text{kg}}{\text{m}^3}$.

An ideal-gas model ($\gamma = 1.4$) is used along with Sutherland’s law for viscosity ($\mu = 1.458 \times 10^{-6} \frac{\sqrt{T^3}}{110.3+T}$) and a constant Prandtl number (Pr) of 0.71. Note that for $T \gg 110.3 \text{ K}$, $\mu \sim T^{0.5}$. Consequently, an exponent of 0.5 is used in a power-law approximation to Sutherland’s law in the empirical relations for displacement and momentum thicknesses of a compressible boundary layer.

Flat Plate Grid: 129 (streamwise) \times 257 (wall normal).

Flat Plate Methodology: (i) a pointwise boundary condition is imposed at the wall—an inviscid (tangency) boundary condition at the first 15 points along the streamwise direction, and a no-slip boundary condition at the remaining points; (ii) the points along each vertical grid line are redistributed using *OUTBOUND*^[10] (off-line precursor of DPLR’s shock alignment scheme) after an initial flowfield computation such that (a) the cell Reynolds number at the wall is unity, and (b) better resolution of the oblique shock is achieved as well; (iii) the flowfield computed on the reclustered grid is post-processed using *BLAYER* to extract edge and integral quantities—displacement and momentum thicknesses.

For an *incompressible* laminar boundary layer on a flat plate with no streamwise pressure gradient, the displacement and momentum thicknesses are:^[5, 8]

$$\delta_{\text{inc}}^* = \frac{1.7208}{\sqrt{Re_x}} x \quad \text{and} \quad \theta_{\text{inc}} = \frac{0.6641}{\sqrt{Re_x}} x \quad \text{where} \quad Re_x = \frac{\rho_e u_e x}{\mu_e} \quad (1)$$

These expressions for an incompressible boundary layer have to be scaled for a compressible boundary layer. To this end, we rely on the reference temperature method developed by Eckert.^[9]

The reference temperature, T^* , is defined as a weighted sum of the edge, wall, and recovery temperatures:

$$T^* = 0.5T_e + 0.5T_w + 0.22r \left(\frac{\gamma-1}{2} \right) M_e^2 T_e \quad (2)$$

where the recovery factor, r , for a laminar boundary layer is:

$$r = \sqrt{Pr} \quad (3)$$

Scaling involves simply replacing the Reynolds number, Re_x , with a new value based on the reference temperature, *i.e.*, Re_x evaluated with density and viscosity evaluated at the reference temperature. The textbook of Hirschel^[11] provides the following expressions (attributed to the work of Simeonides^[12]):

$$\delta_c^* = \delta_{inc}^* \left(-0.122 + 1.122 \frac{T_w}{T_e} + 0.0666 M_e^2 \right) \left(\frac{T^*}{T_e} \right)^{0.5(\omega-1)} \quad (4)$$

and

$$\theta_c = \theta_{inc} \left(\frac{T^*}{T_e} \right)^{0.5(\omega-1)} \quad (5)$$

where the exponent, ω , is 0.5 for Sutherland's law.

Flat Plate Results: The angle of the oblique shock wave was determined from a straight-line fit (not shown) to four shock locations (peak pressures) at the stations $x = 2, 4, 6, 8$ m. as 14.63° , which compares favorably with the theoretical value of 14.48° ($\sin^{-1}(1/M_\infty)$). Figure 9 shows part of the flow field as H/H_∞ contours along with the distributions of δ , δ^* and θ produced by DPLR and the hybrid method of BLAYER.

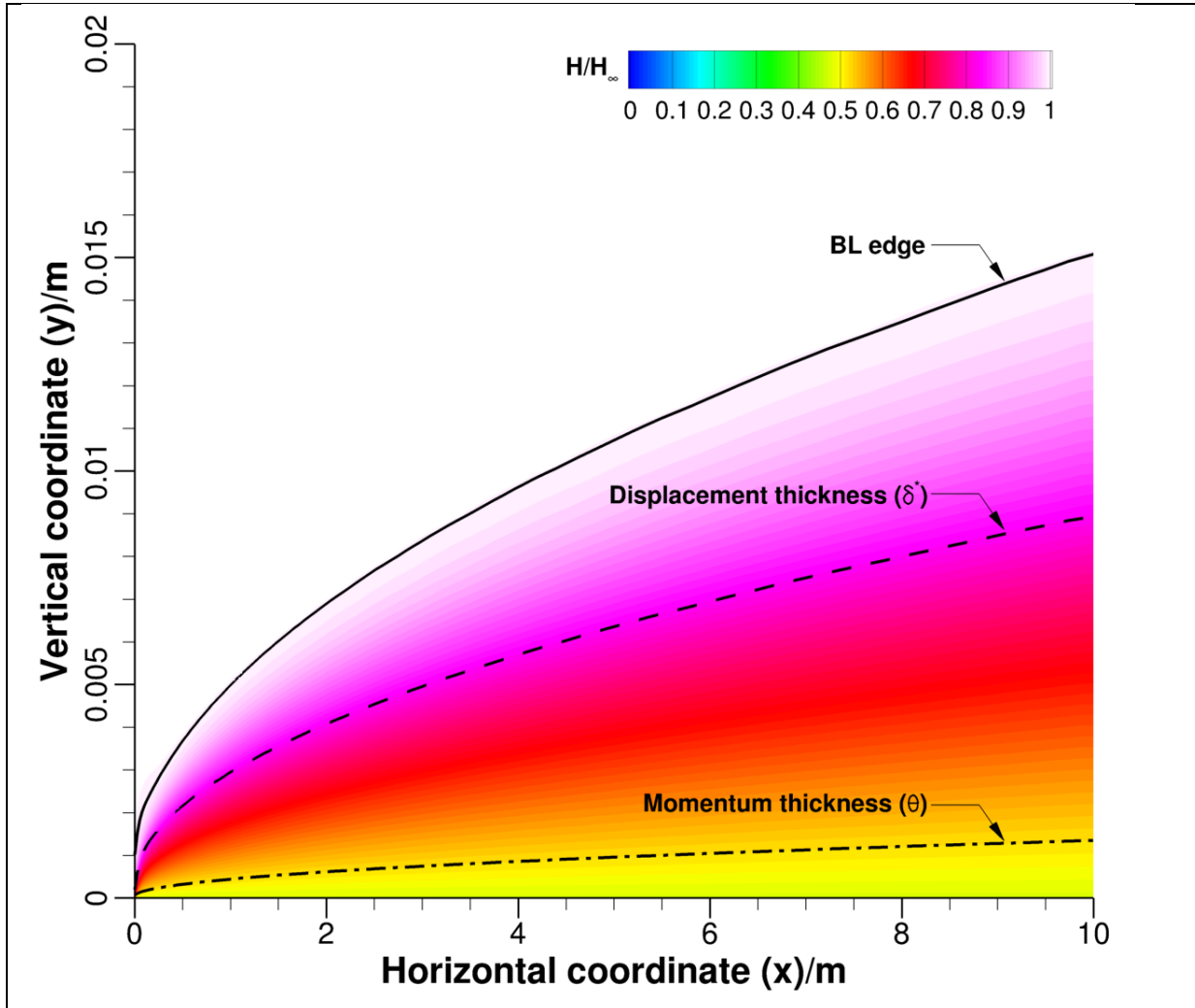


Figure 9. Total enthalpy normalized by freestream total enthalpy, along with results from BLAYER using the hybrid method on a flat plate DPLR solution (compressible). The edge ordinates range from 0 to 0.015 m—roughly two orders of magnitude smaller than the physical distance of the outer boundary of the computational domain. Theoretically, the edge curve is parabolic for the incompressible case.

Figure 10 compares BLAYER results with the compressible corrections to the Blasius equations, showing quite good agreement.

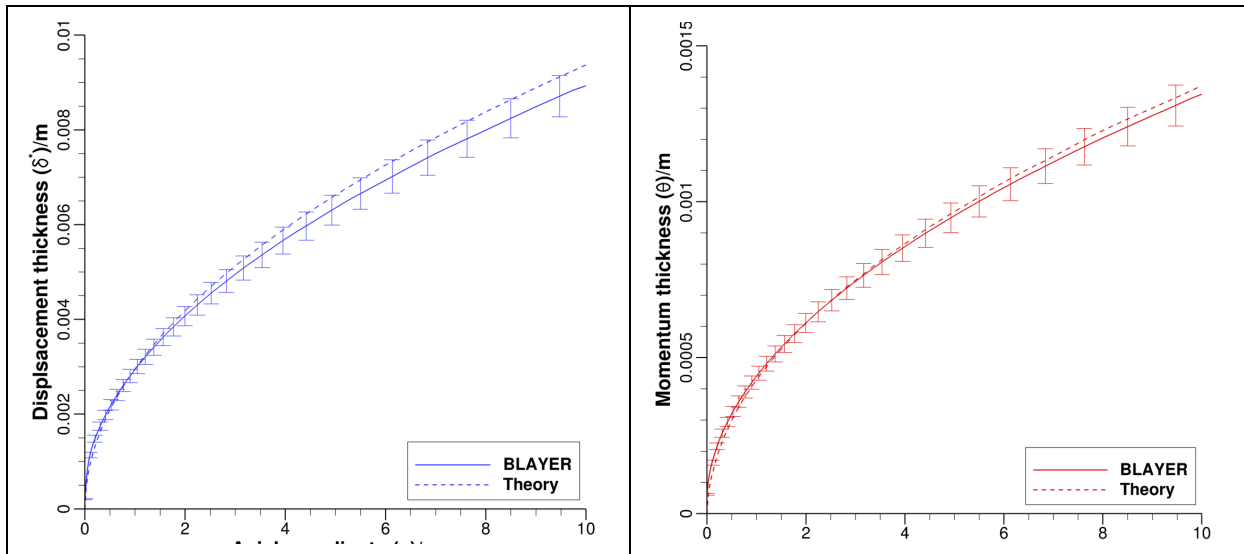


Figure 10. Axial variations of computed flat plate displacement and momentum thicknesses (solid lines) compared with the compressible Blasius forms (dashed lines). The $\pm 5\%$ error bars shown on the computed results are intended to convey the level of disagreement. The more important thickness, θ , is widely used to predict transition of the flow from laminar to turbulent.

Hemisphere Case (2-D axisymmetric, air): An early study compared the pure curvature-based method with the plain 99.5% method for a unit-radius hemisphere at Mach ~ 22 in 7-species air, as in Fig. 11. The right-hand plot shows that the two edge detection methods are indistinguishable here, with the expected smoothness in edge-related quantities. Note that zeros are initially computed for δ^* and θ at the stagnation point (because tangential velocities are all zero along the stagnation line). These zeros are trapped and replaced with extrapolations along the surface by the current version of BLAYER. The free-stream conditions here are: $V_\infty = 7.708$ km/s, $\rho_\infty = 5.3169E-3$ kg/m³, $T_\infty = 300$ K, $Re = 2.101$ million/m, $M_\infty = 22.15$.

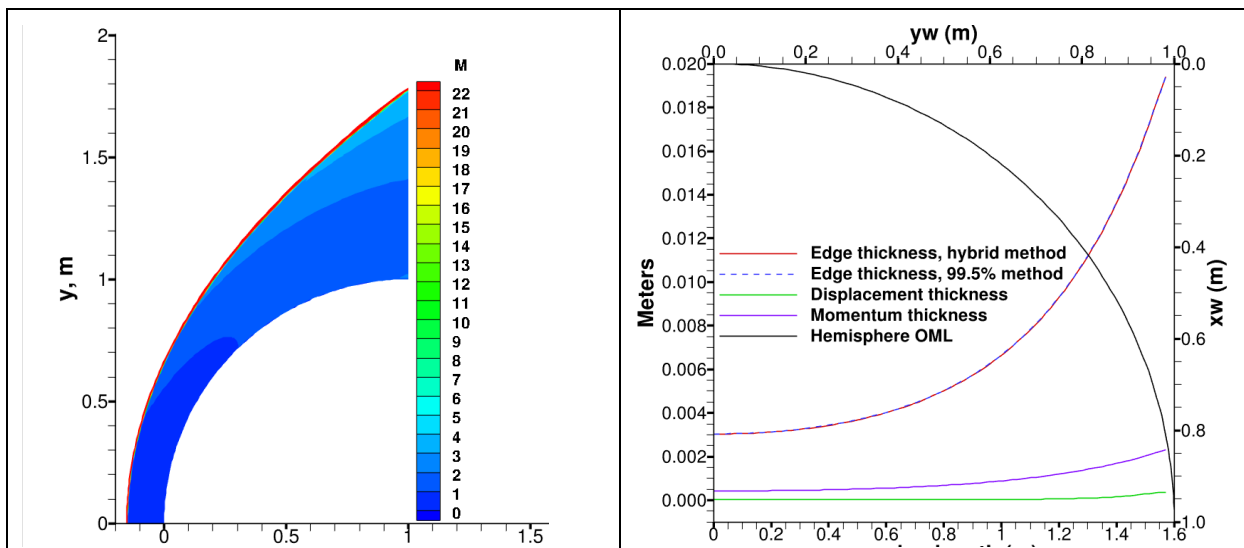


Figure 11. For a hemisphere solution at Mach ~ 22 (left), the curvature-based edge method is indistinguishable from the plain 99.5% method in the right-hand plot. This is a hot-wall/radiative equilibrium laminar case.

Laminar cold wall ($T_{wall} = 300$ K) and fully turbulent (Baldwin-Lomax) cold-wall variations of this hemisphere case are also presented. The different wall boundary conditions have less effect on the various thicknesses computed by BLAYER than might be expected ($T_{wall} = 2000$ - 3000 K for the hot wall case), probably because the boundary layer thicknesses are relatively small at this Reynolds no. See Fig. 12.

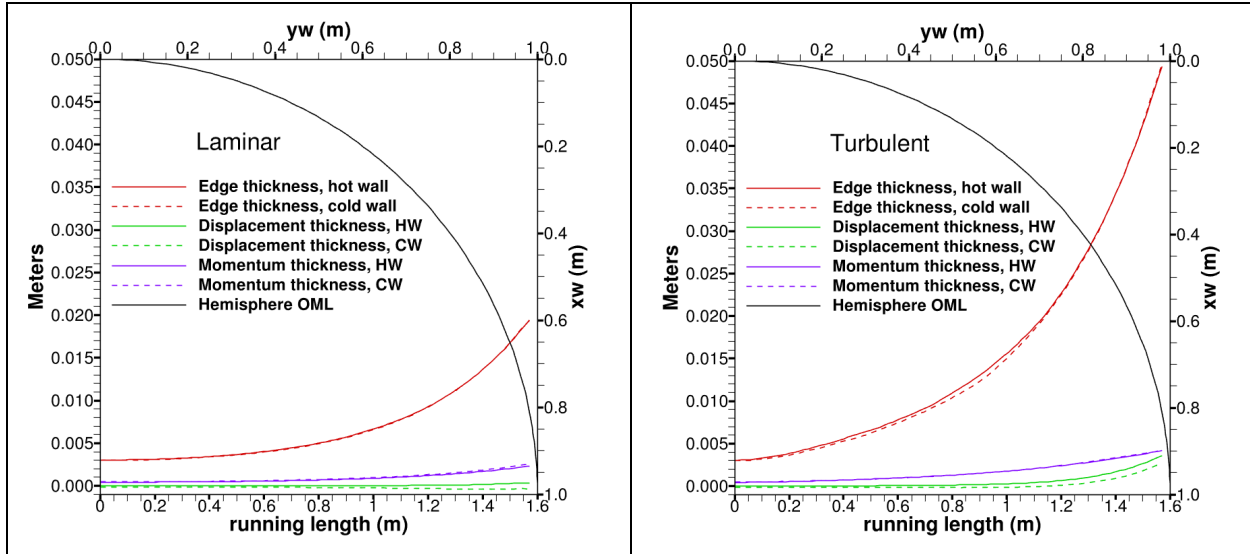


Figure 12. Both laminar and fully turbulent hemisphere solutions for this free stream are insensitive to the wall boundary condition (radiative equilibrium, solid lines, and cold wall/300 K, dashed lines). Displacement thickness is commonly negative at high Reynolds numbers.

The laminar derived quantities Re_θ and Re_{kk} commonly used to predict turbulent transition are compared for cold and hot wall variations in Fig. 13. These predictions are not necessarily inconsistent because Re_θ is used to predict transition on a smooth surface while Re_{kk} predicts transition due to surface roughness. We see that the hot wall case with roughness height $k = 0.1$ mm is unlikely to become turbulent at all ($Re_{kk} < 200$ everywhere) while the cold wall case should transition.

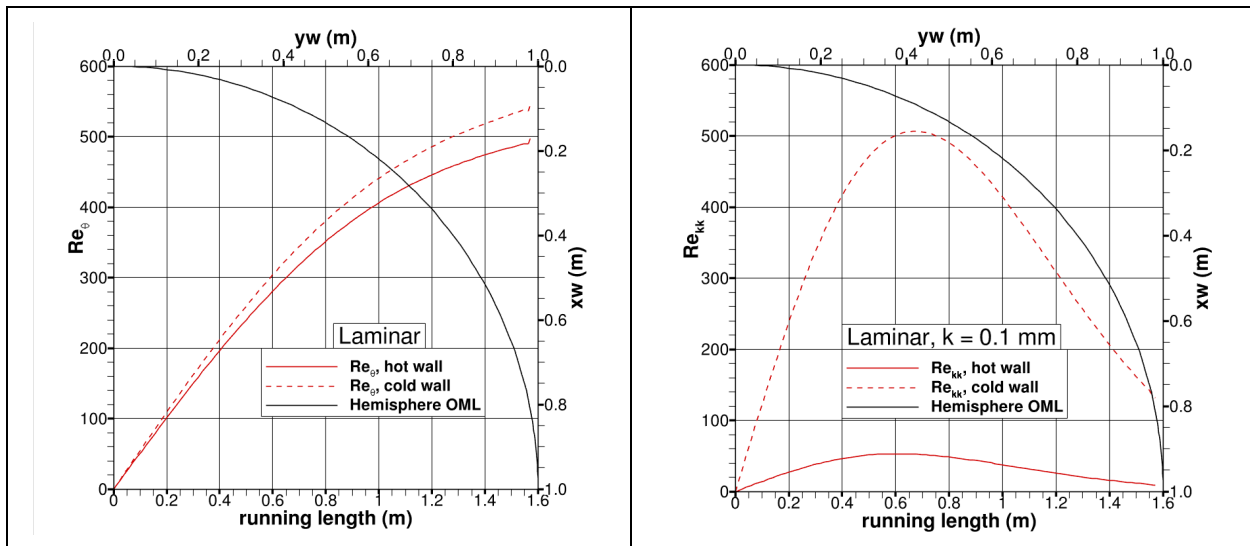


Figure 13. Re_{kk} (on the right) is significantly more affected than Re_θ (on the left) by the wall boundary condition, because Re_{kk} uses viscosity at the wall, not at the edge, and viscosity is sensitive to temperature. See pp. 6-7 for extended use of BLAYER's roughness height input to obtain Re_θ or Re_θ/M_{edge} in place of Re_{kk} . Alternatively, use TECPLOT equations.

Orion Case (3-D flow in air): A 3-D example of boundary layer edge results is shown in Fig. 14, with pleasingly smooth contours in the attached aft body region. The less smooth contours appearing on the forebody would undoubtedly be improved by a further grid alignment with the bow shock.

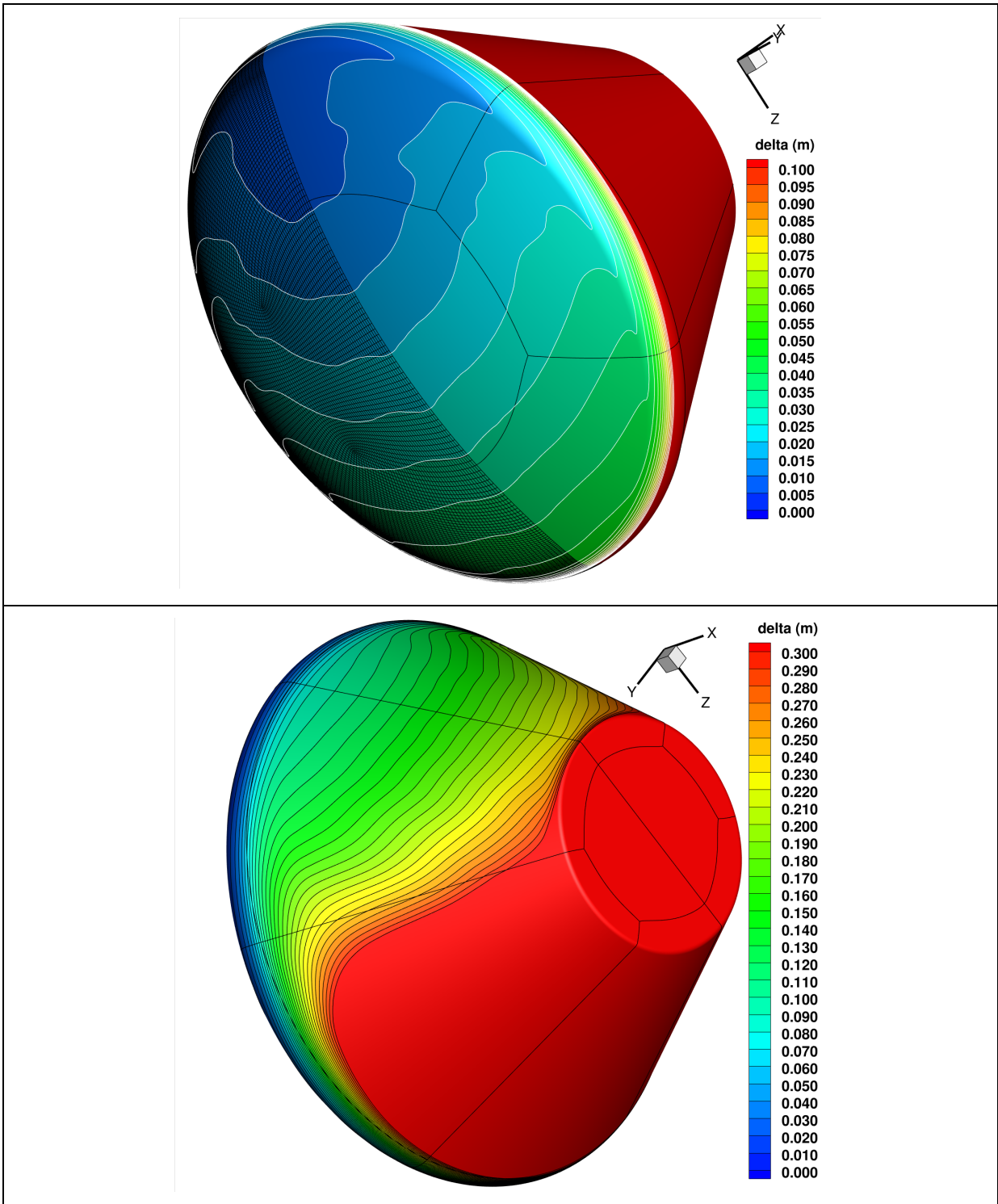
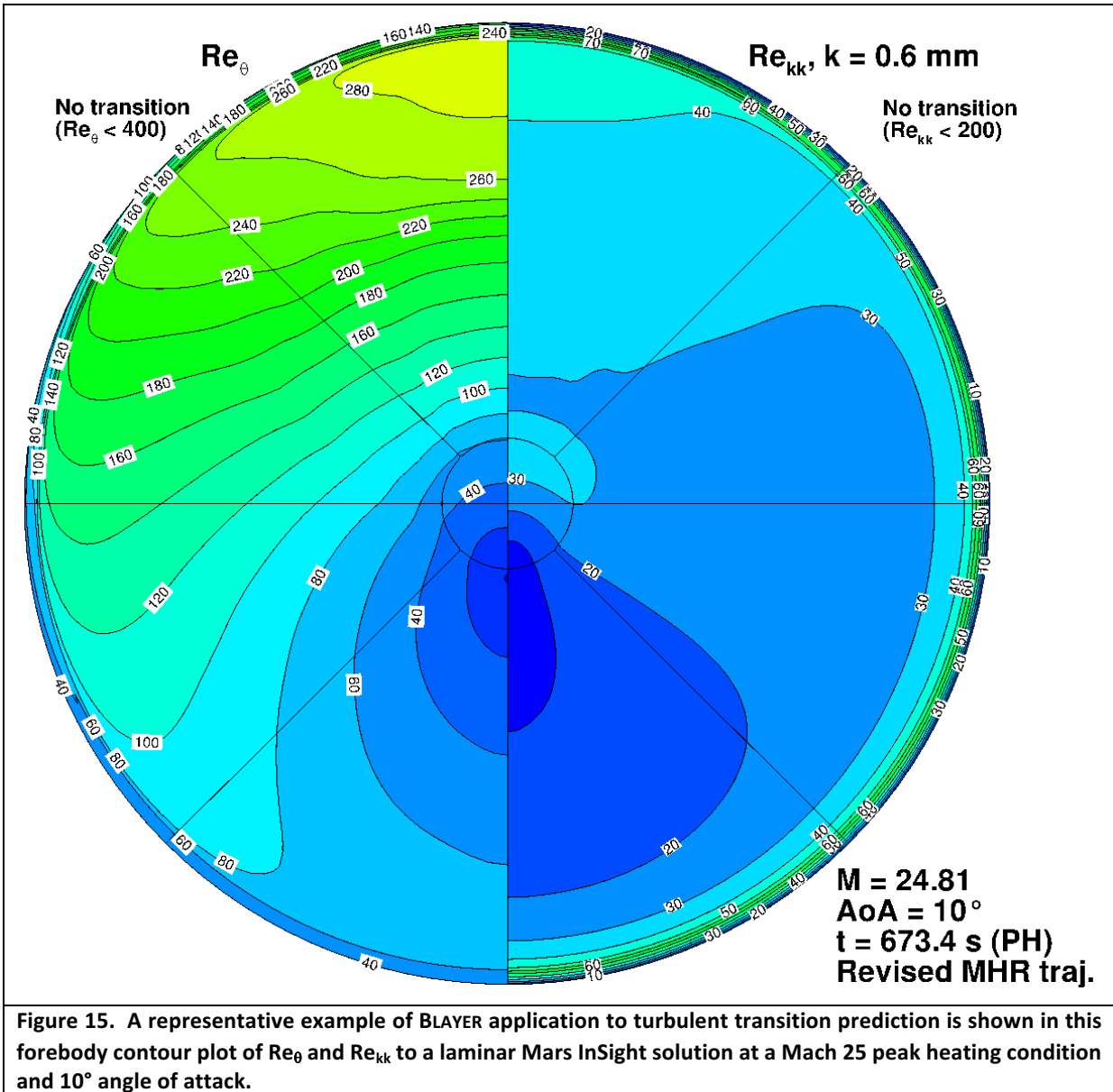


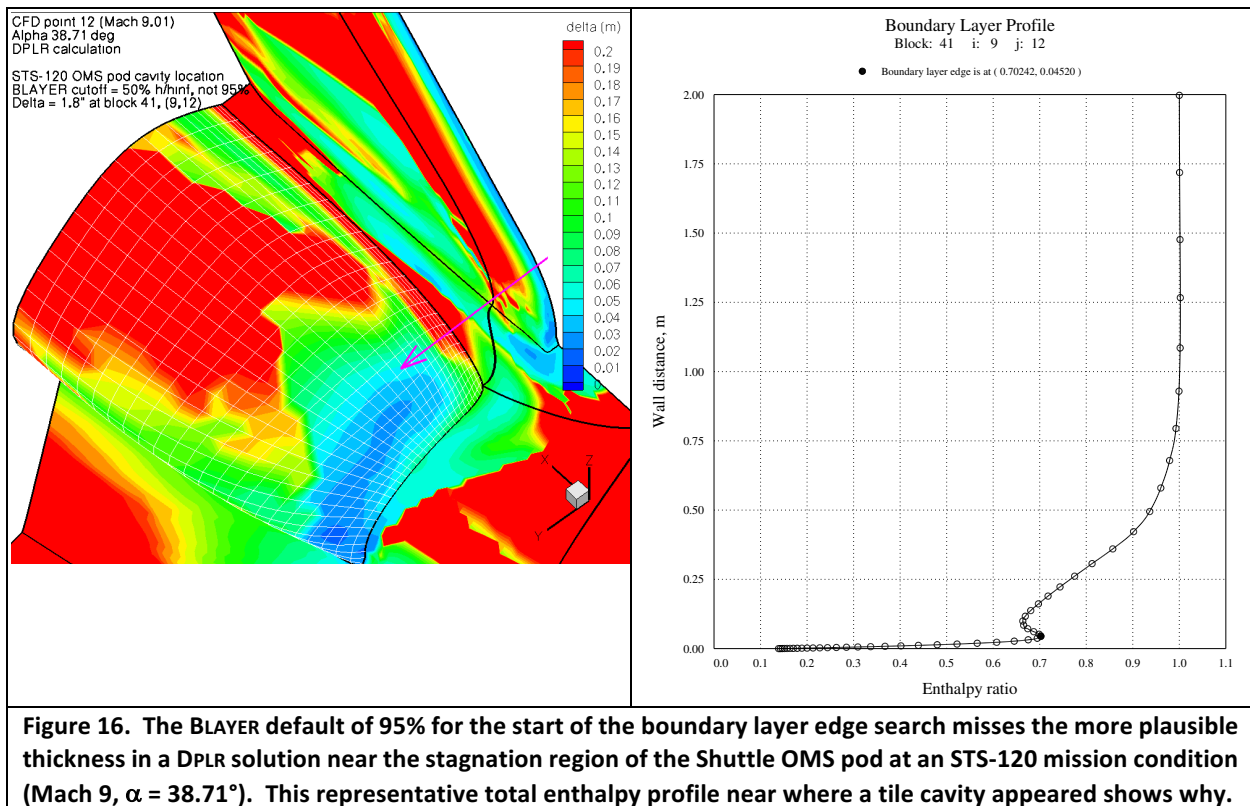
Figure 14. Representative BLAYER behavior is shown for a turbulent (Baldwin-Lomax) Orion case at a high Mach condition. The minor forebody contour irregularities (upper image) are more likely to indicate imperfect grid alignment with the bow shock than non-smooth variation of the boundary layer edge detection scheme. Edge height variation is admirably smooth on the attached region of the aft body in the lower image.

Mars InSight Case (3-D flow in CO₂): Figure 15 illustrates another 3-D application, to laminar-turbulent transition predictions at Mars.



VI. Anomalous Behaviors

Under ordinary circumstances, total enthalpy profiles should not exhibit overshoots or undershoots in the boundary layer region. In practice, anomalous profiles are inevitable, and BLAYER is an attempt to cope with them better than the traditional edge detection method does. Establishing a single set of heuristics to accommodate every possibility, however, remains an ideal yet to be achieved. Apart from the separated flows that are likely within any full-body solution, along with their wake flows, there may be shock-shock interactions such as those produced by the nose of the Shuttle Orbiter at the wing leading edge. The **Shuttle OMS pods** (Orbital Maneuvering System) provide a more tractable example. Even at the high entry angles of attack, they experience their own stagnations points and boundary layers that are not properly captured by BLAYER's default settings. Indeed, the "Hignore" control was introduced with this situation in mind: a value of 50% was found to enable sensible results during STS-120 when some tile damage was observed on the starboard pod, as shown in Fig. 16. Implausibly thick boundary layers are predicted in this region with the standard heuristics, and a sample profile illustrates the reason. For Orion applications, this 95% default cut-off heuristic has proved vulnerable; 98% is now the "Hignore" input employed in Orion post-processing scripts.



Mars InSight Anomaly: A second example shows anomalous results on a perfectly ordinary configuration that can be traced to unexpected travel of shock-related disturbances to the boundary layer region towards the lee-side shoulder of the heat shield. This was first noticed in a plot of the Re_0 distribution for a 70° sphere/cone at angle of attack during a Mars entry. Switching to the traditional 99.5% edge method produced a much cleaner distribution. The simpler method is unaffected by the profile overshoots that turned out to be present (Fig. 17). The odd Re_0 distribution is reflected by similar behavior in the edge thickness and in the momentum thickness (Fig. 18). The contour plot of total enthalpy ratio (shifted form) in Fig. 19 suggests that shock-related effects begin opposite the sphere-cone

tangency point and travel to the lee-side shoulder. Figure 20 confirms that in the region around $r = 0.95$ m, the disturbance does indeed enter the boundary layer. Thus, in this example, the hybrid method is revealing what are really flow solution imperfections rather than suffering from algorithm weaknesses. Note that grid line orthogonality at the wall, grid alignment with the shock, and flow solver convergence were all eliminated as possible sources. A fourth grid alignment made no perceptible difference, while the radial grid line for the illustrated profile was shown to be just 0.5° off body-normal for its full length (see the red grid line in Fig. 19).

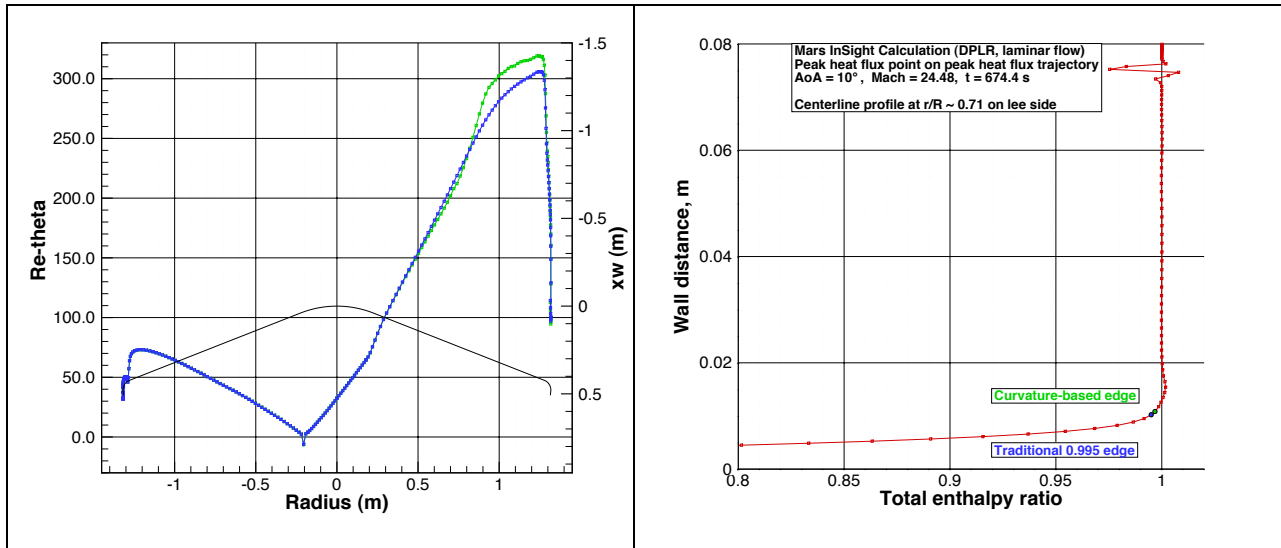


Figure 17. Anomalous behavior of the centerline Re_θ distribution for a Mars InSight solution at Mach 24.5, $\alpha = 10^\circ$, on the lee side. The total enthalpy profile shown is for the body point where the anomaly is greatest near radius = 0.95 m, and it contains an overshoot that moves the edge higher for the hybrid method.

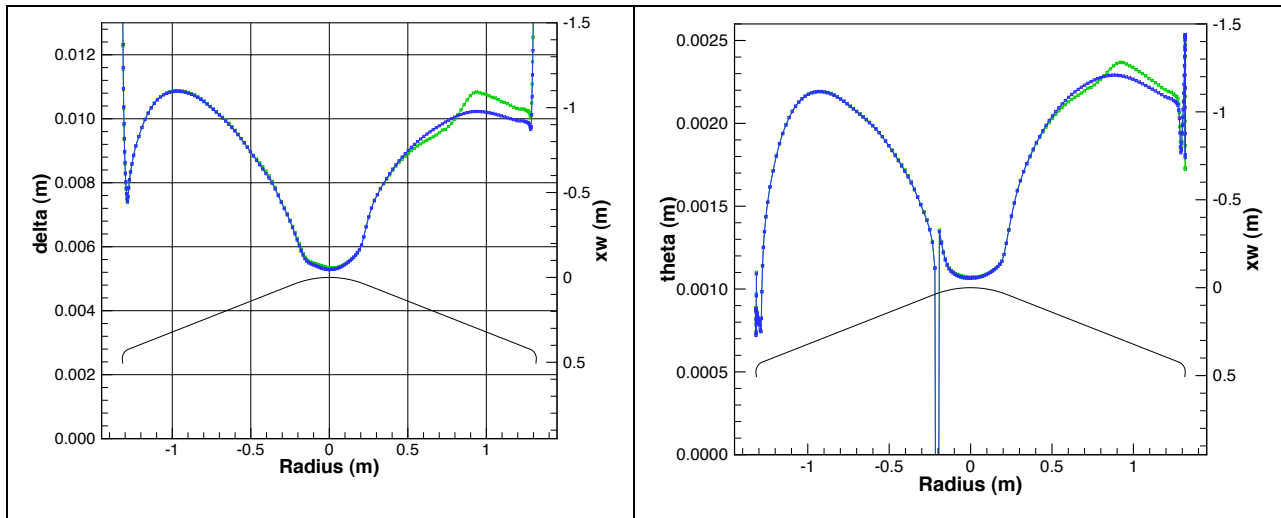


Figure 18. Evidence of profile undershoots and overshoots appears in the edge thickness distribution (left) for the case of Fig. 17. The momentum thickness distribution (right) from the hybrid method is similarly anomalous. Note that the flat-plate-inspired assumptions in the definition of θ break down towards the stagnation point in spite of safeguarding against zero tangential velocity. See Figs. 19 and 20 for evidence that the overshoot region extends into the boundary layer towards the lee-side shoulder.

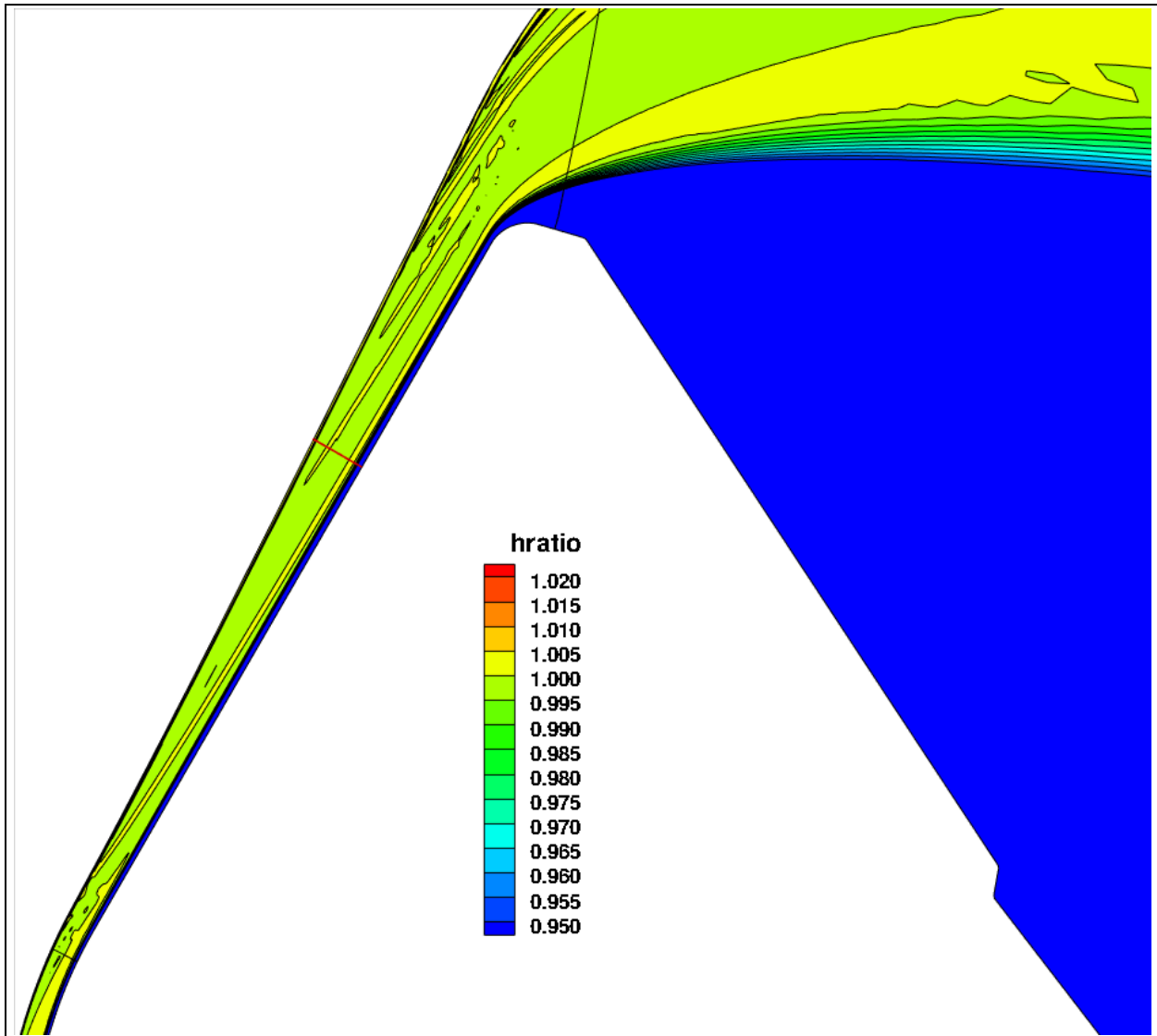


Figure 19. Contours of the shifted form of total enthalpy ratio for the Mars InSight case of Figs. 17 and 18 show a yellow band slightly higher than 1.0 that emanates from the shock opposite the sphere/cone juncture and travels to the boundary layer region of the lee-side shoulder. The red line mid-left is the location of the total enthalpy profile shown in Fig. 17. See also Fig. 20.

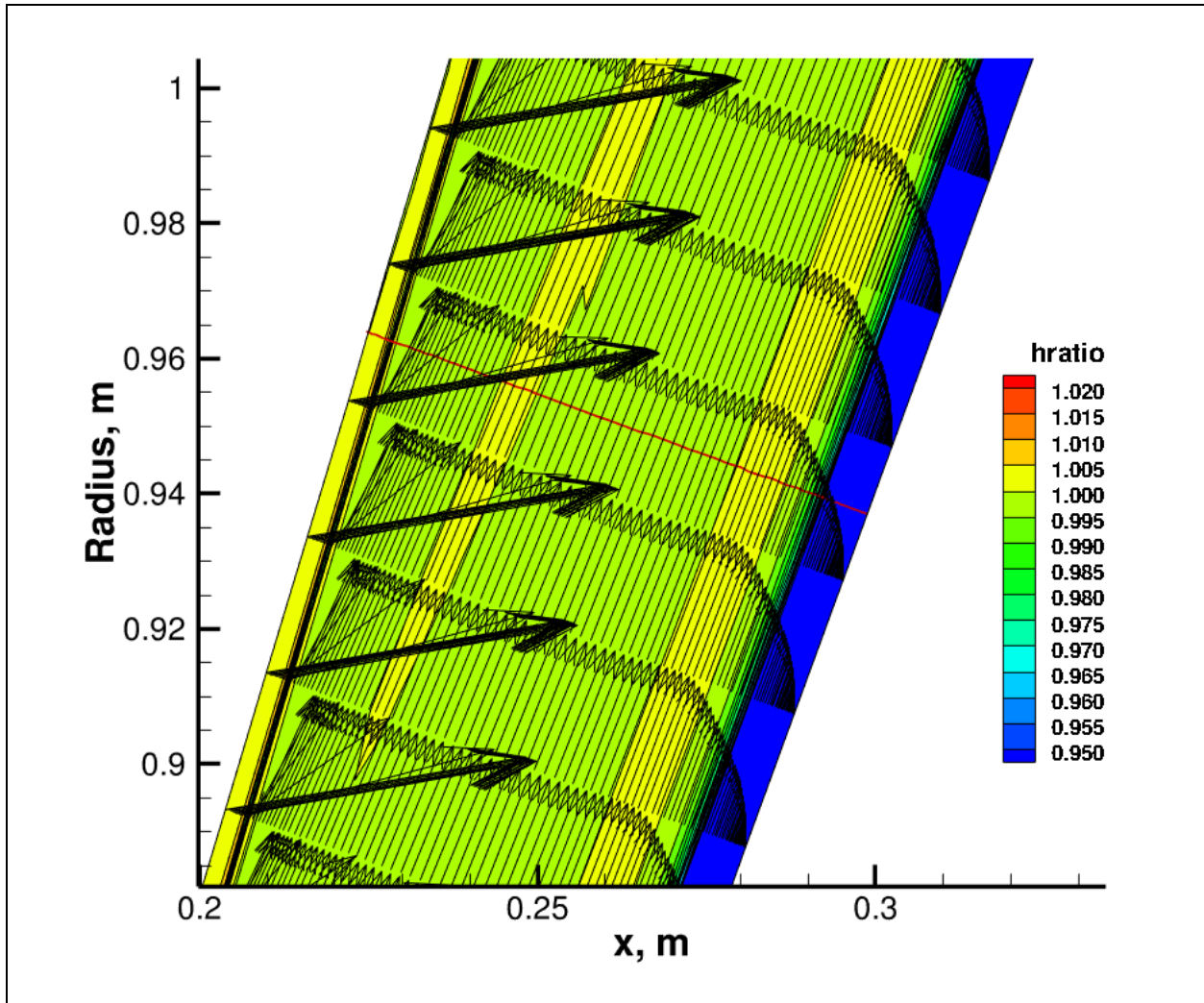
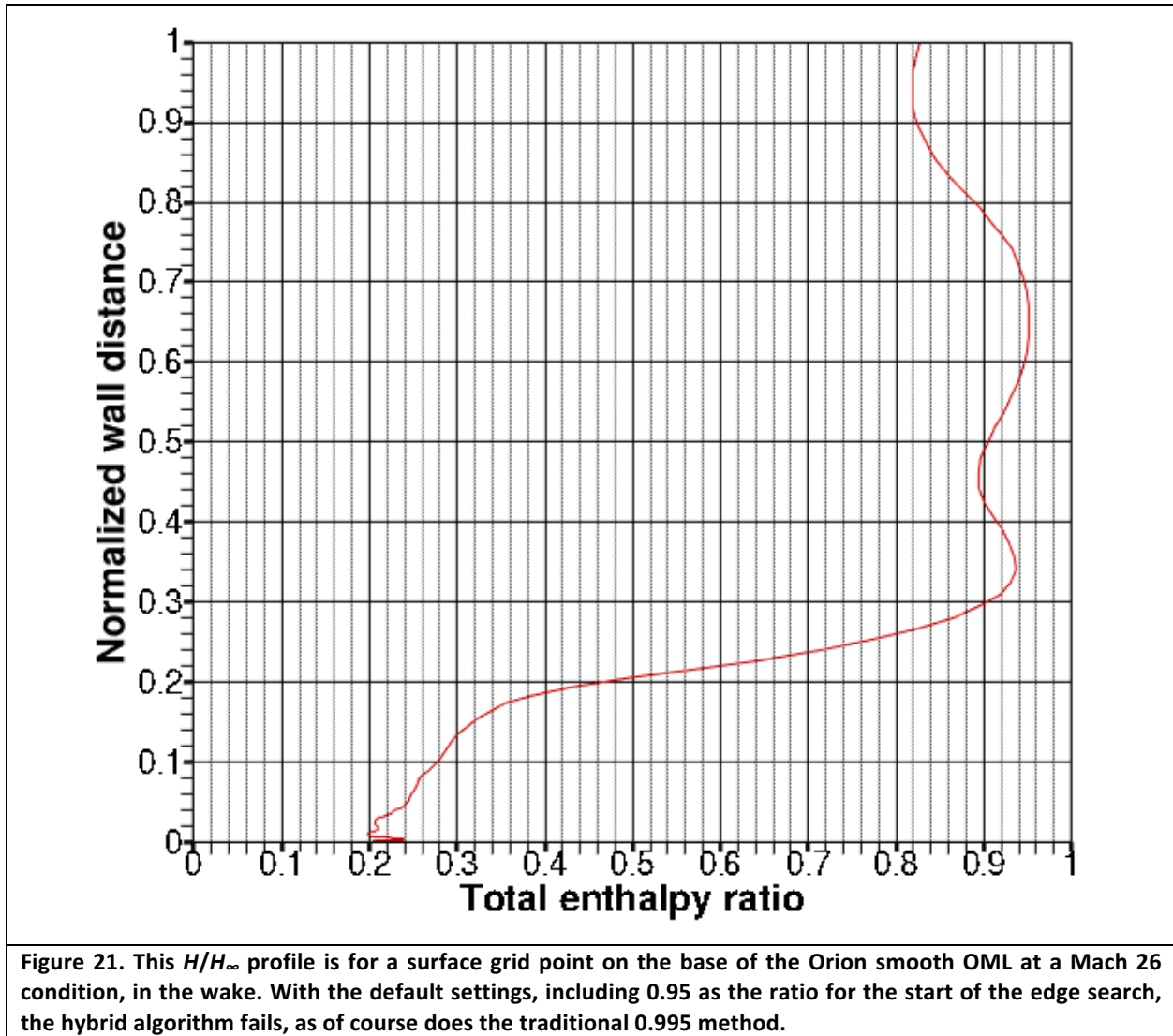


Figure 20. Velocity vectors added to the contours of Fig. 19 confirm that the yellow band slightly exceeding 1.0 does enter the boundary layer in the region near radius = 0.95 m. The flow solution is cell-centered. The red line corresponds to the vertex-centered grid line of the profile shown in Fig. 17.

Edge Detection Failures: Either of the edge detection methods can fail completely for anomalous profiles at what are bound to be aft body points barring some input error. (Among other possibilities, long off-body grid lines in the wake tend to violate some of the BLAYER assumptions.) BLAYER reports edge detection failures by writing the first offending profile ($x,y,z,t,hratio$) to standard output for each grid block, and reporting the total count of troublesome profiles for that block. Results for some uncertain “kedge” index will still be produced and the run proceeds so that plotting can still be performed. Figure 21 shows a profile for which the hybrid algorithm failed with the 95% default for “Hignore” because the total enthalpy ratio is less than the cut-off value everywhere.



N.B.: Extremely tight grid spacing occasionally explains BLAYER misbehavior. This is because, by default, the utility determines which face of each grid block has the smallest average off-face grid spacing and permutes indices if necessary to make that face be the $k = 1$ face as assumed by the ensuing steps. (Very tight resolution of the shock, for instance, has been observed to trip this test.) The work-around is to use ancillary control file `blayer.inp.2` to specify the correct face for each block. See page 7. Note that even for 2-D solutions, face 5 should be specified for the $j = 1$ face, because such solutions are treated as being dimensioned $(ni,1,nj)$, not (ni,nj) .

Finally, an excerpt from the BLAYER source code history section illustrates the type of practical difficulty encountered by the curvature-based approach in the edge region where gradients are highest:

```
!      06/24/08   Discontinuities towards the Shuttle wing tip were
!                  traced to profiles that straighten up short of 1.0
!                  before achieving 1.0.  This means the heuristic
!                  size of the neighborhood of the peak curvature
!                  can include ~1.0 for one profile but not for a
!                  neighboring profile.  Stage 2 of the edge method
!                  then seeks 99.5% of quite different peaks in those
!                  neighborhoods.  Use of 99.5% means even small
!                  changes lead to large differences in edge thickness
!                  when the profile is so steep.  Mike Olsen suggested
!                  using 95% to reduce the effect greatly, but then
!                  all edge-related quantities would be significantly
!                  lower everywhere.  After much pondering, we stay
!                  with 99.5%, and accept that wing tip regions are of
!                  limited interest anyway, even on the wind side.
```

The interested reader is reminded that the BLAYER source code^[13] is thoroughly documented in-line, and should be consulted when questions arise.

VII. Acknowledgments

The BLAYER software was implemented at NASA Ames Research Center under TSA Aerothermodynamics Branch contracts with ELORET Corporation (NNA04BC25C) and ERC, Inc. (NNA10DE12C), and funded mostly by the Shuttle RTF (Return to Flight) program. At the time of writing this User Guide, the authors are contractors with AMA, Inc. at NASA ARC (Contract NNA15BB15C). Helpful review comments from Ryan McDaniel, Michael Olsen, Michael Wilder (NASA ARC) and Brett Cruden (AMA, Inc. at NASA ARC) are gratefully acknowledged.

VIII. References

- [1]. TECPLOT (more precisely TECPLOT 360) is one of a family of data visualization and analysis tools developed by Tecplot, Inc., Bellevue, WA. TECPLOT is a de facto standard at NASA.
- [2]. https://en.wikipedia.org/wiki/PLOT3D_file_format
- [3]. Wright, Michael J., White, Todd R., Mangini, Nancy, “Data Parallel Line Relaxation (DPLR) Code User Manual: Acadia – Version 4.01.1.”
- [4]. https://en.wikipedia.org/wiki/STS-114#In-flight_repair
- [5]. White, Frank M., *Viscous Fluid Flow*, 3rd Edition, McGraw-Hill, 2005.
- [6]. Committee on Data for Science and Technology (CODATA); <https://www.nist.gov/programs-projects/codata-values-fundamental-physical-constants>
- [7]. Reda, Daniel C., “Review and Synthesis of Roughness-Dominated Transition Correlations for Reentry Applications,” *Journal of Spacecraft and Rockets*, Vol. 39, No. 2, Mar-Apr 2002.
- [8]. Schlichting, H., *Boundary-layer Theory*. Springer 2004.
- [9]. Eckert, E. R. G., “Engineering Relations of Friction and Heat Transfer to Surfaces in High-Velocity Flow,” *J. Aero. Sci.*, Vol. 22, No. 8, 1955, pp. 585-587.
- [10]. David A. Saunders and Seokkwan Yoon, “An Approach to Shock Envelope Grid Tailoring and Its Effect on Reentry Vehicle Solutions,” AIAA Paper 2007-207, 2007.
- [11]. Hirschel, E. H., *Basics of Aerothermodynamics. Vol. 204 of Progress in Astronautics and Aeronautics*, AIAA, 2005.
- [12]. Simeonides, G., “Hypersonic Shock Wave Boundary Layer Interactions over Compression Corners,” Doctoral Thesis, University of Bristol, U. K., 1992.
- [13]. <https://sourceforge.net/projects/cfdutilities>

REPORT DOCUMENTATION PAGE			Form Approved OMB No. 0704-0188		
Public reporting burden for this collection of information is estimated to average 1 hour per response, including the time for reviewing instructions, searching existing data sources, gathering and maintaining the data needed, and completing and reviewing this collection of information. Send comments regarding this burden estimate or any other aspect of this collection of information, including suggestions for reducing this burden to Department of Defense, Washington Headquarters Services, Directorate for Information Operations and Reports (0704-0188), 1215 Jefferson Davis Highway, Suite 1204, Arlington, VA 22202-4302. Respondents should be aware that notwithstanding any other provision of law, no person shall be subject to any penalty for failing to comply with a collection of information if it does not display a currently valid OMB control number. PLEASE DO NOT RETURN YOUR FORM TO THE ABOVE ADDRESS.					
1. REPORT DATE (DD-MM-YYYY) 01-2018		2. REPORT TYPE Technical Memorandum		3. DATES COVERED (From - To)	
4. TITLE AND SUBTITLE BLAYER User Guide			5a. CONTRACT NUMBER NNA15BB15C		
			5b. GRANT NUMBER		
			5c. PROGRAM ELEMENT NUMBER		
6. AUTHOR(S) David A. Saunders and Dinesh K. <u>Prabhu</u>			5d. PROJECT NUMBER		
			5e. TASK NUMBER		
			5f. WORK UNIT NUMBER		
7. PERFORMING ORGANIZATION NAME(S) AND ADDRESS(ES) AMA, Inc. Hampton, Virginia at Ames Research Center Moffett Field, CA 94035-1000			8. PERFORMING ORGANIZATION REPORT NUMBER		
9. SPONSORING / MONITORING AGENCY NAME(S) AND ADDRESS(ES) National Aeronautics and Space Administration			Ames Research Center Moffett Field, CA 94035-1000		
			10. SPONSOR/MONITOR'S ACRONYM(S) NASA		
12. DISTRIBUTION / AVAILABILITY STATEMENT Unclassified—Unlimited Subject Category: 34, 61 Availability: NASA CASI (301)621-0390			11. SPONSOR/MONITOR'S REPORT NUMBER(S) NASA/TM-2018-219749		
			13. SUPPLEMENTARY NOTES Point of Contact: David.A.Saunders@NASA.gov or Dinesh.K.Prabhu@NASA.gov		
14. ABSTRACT A software utility employed for post-processing computational fluid dynamics solutions about atmospheric entry vehicles is described as a supplement to the documentation within the source code. This <u>BLAYER</u> application and its ancillary utilities are in the public domain at https://sourceforge.net/projects/cfdutilities/ . <u>BLAYER</u> was developed at NASA Ames Research Center in support of the <u>DPLR</u> (Data Parallel Line Relaxation) flow solver. Its underlying algorithm has since been incorporated by others into the <u>LAURA</u> and <u>US3D</u> flow solvers at NASA Langley Research Center and the University of Minnesota respectively. The essence of the algorithm is to locate the boundary layer edge by seeking the <i>peak curvature</i> in a total enthalpy profile. Turning that insight into a practical tool suited to a wide range of possible profiles has led to a <i>hybrid</i> two-stage method. The traditional method—location of (say) 99.5% of free-stream total enthalpy—remains an option, though it may be less robust.					
15. SUBJECT TERMS Boundary layer, CFD, Computational Fluid Dynamics, hypersonic flow, real gas, atmospheric entry					
16. SECURITY CLASSIFICATION OF:			17. LIMITATION OF ABSTRACT	18. NUMBER OF PAGES	19a. NAME OF RESPONSIBLE PERSON
a. REPORT Unclassified	b. ABSTRACT Unclassified	c. THIS PAGE Unclassified	Unclassified	28	David A. Saunders
			19b. TELEPHONE NUMBER (include area code) (650) 604-1480		

Standard Form 298 (Rev. 8-98)
Prescribed by ANSI Std. Z39.18